Recent Advances in the Chemistry and Application of SF5-Compounds

Mariam Abd El Sater, Nicolas Blanchard, Vincent Bizet, Lucas Popek

Recent Advances in the Chemistry and Application of SF_5-Compounds

Mariam Abd El Sater
Lucas Popek
Nicolas Blanchard
Vincent Bizet*

Université de Haute-Alsace/Université de Strasbourg, Laboratoire d'Innovation Moléculaire & Applications (LIMA), UMR CNRS 7042, Institut de Recherche Jean-Baptiste Donnet, 3bis rue Alfred Werner, 68057 Mulhouse, France
vbizet@unistra.fr

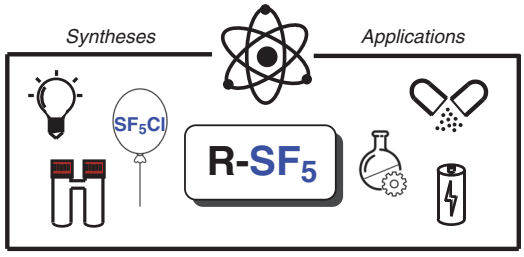

DOI: 10.1055/a-2383-6620; Art ID: SS-2024-07-0305-SR

Abstract This review article outlines the literature from 2022 to 2024 covering developments in SF_5 chemistry. Recent synthetic methodologies of SF_5-containing building blocks are reported. These methods include the synthesis of SF_5Cl and its use in pentafluorosulfanylation reactions and oxidative fluorination reactions. Moreover, the reactivity of SF_5-alkynes as versatile platform to access new SF_5-compounds is described. Finally, the effects of the SF_5 moiety are highlighted according to its application in different fields, such as biological/medicinal chemistry, catalysis, and material sciences.

Key words SF_5Cl, pentafluorosulfanylation, SF_5 building blocks, oxidative fluorination, medicinal chemistry, materials science, catalysis

1 Introduction

Often seen as an exotic perfluorinated motif, the pentafluorosulfanyl group (SF_5) has become of great interest in the last few decades as a potent surrogate of the trifluoromethyl group (CF_3). The SF_5 moiety, with its octahedral geometry around sulfur, is sterically superior to CF_3 but smaller than the *tert*-butyl substituent. Additionally, its high electronegativity (3.65 vs 3.36 for CF_3) associated with its high lipophilicity make this group of special interest for life and material sciences applications.[1] Aromatic SF_5-compounds are hydrophobic and hydrolytically more stable than CF_3 analogues. Moreover, preliminary biological studies have shown that SF_5-compounds could be biodegraded by bacteria, offering a potential alternative to the perfluoro- and polyfluoroalkyl substances, so called PFAS such as CF_3.[2] The history began in 1950 with the preparation of trifluoromethylsulfur pentafluoride (CF_3SF_5) by Cady and Silvey,[3a] and then in 1960 Roberts and Ray prepared SF_5Cl, the most powerful pentafluorosulfanylation reagent until now.[3b] Simultaneously, Sheppard reported the first access to Ar-SF_5 compounds from thiols in the presence of AgF_2 combined with an oxidant.[3c] Efforts were amplified until the milestone discovery of Dolbier's Et_3B-catalyzed radical-chain-type chloropentafluorosulfanylation of double and triple bonds.[4] A blossoming of reports then appeared on oxidative fluorination that developed new synthetic methodologies in order to access aliphatic and aromatic SF_5-compounds, respectively. All these works were exhaustively reviewed in 2015,[5] and then again in 2022.[1,6] However, this field of research is evolving very fast and it is now necessary to take stock and identify next challenges. Herein, recent achievements in the synthesis and applications of SF_5-containing molecules from 2022 to 2024 are reported.

2 Access to SF_5-Containing Building Blocks

2.1 By Means of SF_5Cl

Nowadays, the chain radical addition of SF_5Cl to unsaturated molecules, especially alkenes and alkynes, is the most used method to prepare aliphatic SF_5-containing compounds. Several reports have been published describing different variants of the initial Dolbier's method.

From the left to the right, Dr. Mariam Abd El Sater, Lucas Popek, Dr. Nicolas Blanchard, and Dr. Vincent Bizet. **Vincent Bizet** obtained his Ph.D. degree in 2012 from the INSA of Rouen working on organofluorine chemistry and ruthenium catalysis. In the same year, he was awarded an Alexander von Humboldt postdoctoral fellowship and joined the RWTH Aachen University to work on sulfoximine chemistry. In 2014, he joined the University of Geneva for a second postdoctoral stay to develop palladium-catalyzed asymmetric transformations. In 2016, Dr. Bizet was appointed as CNRS researcher and he joined the LIMA laboratory (UMR 7042 CNRS) located in Mulhouse, and he completed his habilitation in 2022. His research interests are in SF_5 chemistry, homogeneous catalysis, heterocyclic chemistry, asymmetric synthesis, and fluorine and sulfur chemistry.

In 2022, Paquin and co-workers reported the photoinitiated *anti*-hydropentafluorosulfanylation of terminal alkynes mediated by SF_5Cl in the presence of $(TMS)_3SiH$ as a hydrogen atom donor.[7] This method allowed the selective generation of the (*Z*)-(alk-1-enyl)pentafluoro-λ^6-sulfanes (*Z*/*E* >85:15), a previously unknown geometrical isomer. Various reaction conditions were examined to optimize the reaction and obtain the desired alkenes as the major product; $(TMS)_3SiH$ was the best hydrogen atom donor (HAD) in Et_2O along with the portionwise addition of SF_5Cl, which seemed to be crucial for a better selectivity. Next, the scope was evaluated; the method tolerated substrates with various functional groups; substrates containing a free amine or an internal alkyne were unsuitable (Scheme 1a). The proposed mechanism involves the generation of the SF_5 radical by the photoinduced homolytic dissociation of SF_5-Cl. The SF_5 radical adds to the alkyne to produce a vinylic radical. This intermediate react with SF_5Cl via a HAT pathway with $(TMS)_3SiH$ to afford the desired product. The DFT calculations highlighted that the selectivity is due to the intrinsic preference of SF_5-substituted vinylic radicals to adopt a *cis* geometry, and to the reduced distortion in the transition structures.

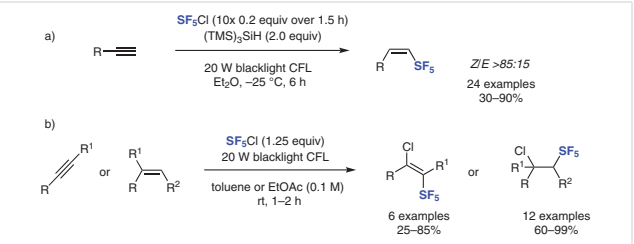

Scheme 1 Photoinitiated *anti*-hydropentafluorosulfanylation (a) and chloropentafluorosulfanylation (b) of terminal alkynes

Their work continued in 2023 with the light activation of SF_5Cl, again using a 20 W blacklight compact fluorescent lamp (CFL) (λ_{max} = 370 nm) in the absence of any other reagent for the atom transfer radical addition to alkenes and alkynes.[8] Optimization of the reaction conditions varying amount of SF_5Cl, temperature, solvent, concentration, and reaction time and an investigation of the scope of different alkenes and alkynes afforded the desired products in good yields (Scheme 1b).

Usually, access to SF_5-alkynes is mainly achieved via a two-step addition of SF_5X (X = Cl, Br) followed by a dehydrohalogenation reaction in basic conditions. Therefore, uncovering alternative efficient and more practical methods to obtain substituted SF_5-alkynes remains highly desirable. In this context, in 2022 the Qing group reported the preparation of substituted SF_5-alkynes from the light-promoted radical reaction of SF_5Cl with ethynylbenziodoxolone (EBX) reagents. Several alkynyliodonium salts were prepared and treated with SF_5Cl in the presence or absence of blue light;[9] improved yields were obtained in the presence of blue LEDs

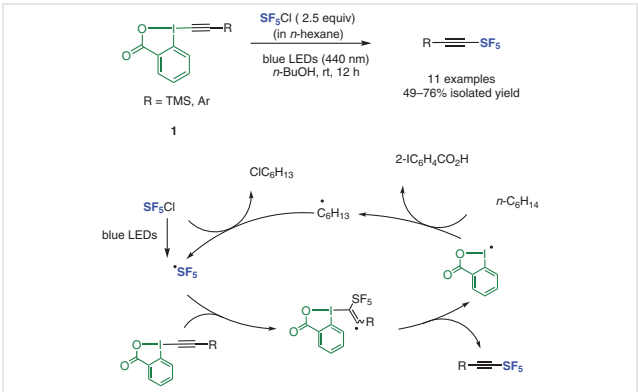

Scheme 2 The radical reaction of ethynylbenziodoxolone (EBX) reagents with pentafluorosulfanyl chloride to access SF_5-alkynes

(440 nm). Moreover, with **1** as the best EBX reagent, a screening of additives and the solvent permitted the scope of the substrates to be examine and finally 11 alkynes were achieved in good yields (Scheme 2). The proposed mechanism relied on the generation of the SF_5 radical upon photoirradiation of SF_5Cl, followed by its addition to the triple bond of the EBX reagent and subsequent elimination of the adduct to afford SF_5-alkynes and the benziodoxole radical. The latter might abstract hydrogen atom from *n*-hexane, the obtained hexyl radical reacts with SF_5Cl to deliver hexyl chloride and regenerate the SF_5 radical.

Following a similar strategy, in 2021 the Qing group reported SF_5Cl addition to diazo compounds leading to the direct preparation of α-SF_5 ketones and esters,[10] then in 2022 they developed a three-component radical addition reaction of SF_5Cl, alkenes, and diazo compounds to afford α-alkyl-α-SF_5 carbonyl compounds.[11] In this case, a carbon radical obtained from the reaction of SF_5Cl with the diazo partner adds to the alkene to form a new carbon radical followed by Cl atom trapping to afford the desired product (Scheme 3).

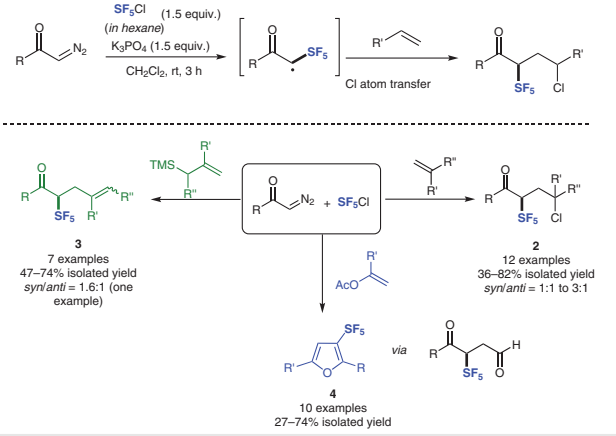

Scheme 3 Three-component reaction of SF_5Cl, alkenes, and diazo compounds for the synthesis of alpha-SF_5-ketones and 3-SF_5-furan

The reaction proceeded in the presence of K_3PO_4 in dichloromethane at room temperature. The scope was explored with various diazo compounds and alkenes affording the corresponding α-alkyl-α-SF_5 carbonyl compounds **2** with moderate yields. While the reaction with hindered 1,1-disubstituted alkenes requires 40 °C, it failed to occur with styrene, cyclohexene, electron-deficient phenyl acrylate, and alkynes. Moreover, α-allyl-α-SF_5 carbonyl compounds **3** were obtained when allyltrimethylsilane was used as the alkene via the elimination of Me_3SiCl during the purification by chromatography. Interestingly, access to SF_5-furans **4** was also possible by using vinyl acetates as alkene component. In this case, 2-SF_5-1,4-dicarbonyl compounds were obtained first and then cyclized in the presence of AgOTf and KF to the desired 3-SF_5-furans in moderate to good yields.

As mentioned before, the introduction of SF_5 moiety, especially for aliphatic molecules, is limited to the use of SF_5X notably with unsaturated compounds. Unlike SF_5Cl and SF_5Br, SF_5I remains uncovered. Noteworthy, thanks to the important difference in electronegativity in case of SF_5I, research efforts were dedicated to the access to SF_5 anion. To date, the chemistry of SF_5^- remains a big challenge and it is yet impossible to introduce SF_5 by means of this anion due to its highly exergonic dissociation into SF_4 and fluoride.

In this regard, Bizet, Cahard, and co-workers tried to prepare SF_5I and to study its reactivity in the novel iodopentafluorosulfanylation of alkynes.[12] They began their study by performing the iodopentafluorosulfanylation of alkynes using a hexane solution of SF_5Cl in the presence of KI. Optimization of the reaction afforded the iodo-2-SF_5 alkene **5** as the major product with respect to the undesired chloro- and diiodoalkenes. The optimized conditions used 3 equivalents of SF_5Cl with KI (4 equiv.) in THF at –78 °C and more interestingly in the presence of one equivalent of 18-crown-6-ether to complex the potassium ion (Scheme 4). The scope of the reaction was investigated using aryl- and alkyl-substituted acetylenes. Arylacetylenes with electron-withdrawing groups (CF_3, OCF_3, and halogens) and phenylacetylene gave products **5** in 51–>98%. 4-Formylphenylacetylene gave the corresponding product **5** in moderate yield, while 4-nitrophenylacetylene, containing a strong electron-withdrawing group, inhibits the reaction. Arylacetylenes bearing electron-donating groups gave moderate yields; fused ring systems gave poor yields. Alkyl-substituted acetylenes had lower reactivity and selectivity whereby the chloroalkenes were obtained together with the corresponding iodo products **5**. In all cases, the *E* isomer was selectively formed, as confirmed by XRD analysis. A mechanistic study supported by DFT calculations by Legault was performed in order to uncover the intermediates and understand the origin of reactivity. From both experiments and DFT calculations, it was concluded that access to SF_5I is thermodynamically impossible and anionic iodopentafluorosulfanylation is not operative even though the formation of SF_5^- was confirmed by ^{19}F NMR. It was calculated that the addition of SF_5^- would lead the opposite regioisomer and that the reaction takes place following a radical process with the *in situ* generation of $SF_5^{\bullet}$ and $I^{\bullet}$ radicals.

In 2024, Bizet, Cahard, and co-workers reported an activator-free radical chloropentafluorosulfanylation of alkynes using SF_5Cl alone in THF as solvent.[13] They proposed that SF_5

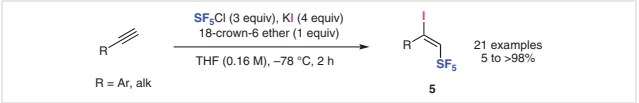

Scheme 4 Access to 2-iodo-1-SF_5-alkenes using SF_5Cl and KI

radicals are generated thanks to traces of hydroperoxides present in the ethereal solvent. To prove their hypothesis, the chloropentafluorosulfanylation of phenylacetylene was carried out in THF at –40 °C. Low temperature was crucial to minimize the polymerization of THF. The desired *E*-2-chloro-1-SF_5-alkenes were obtained as the major product (Scheme 5). It was shown that undistilled solvents are slightly less efficient, light is not necessary, and solubilized oxygen might not play any role in this reaction. Comparison between this method and the previous ones allows its wider versatility and selectivity to be confirmed.

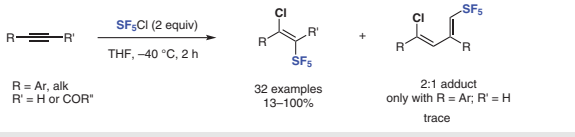

Scheme 5 Activator-free radical chloropentafluorosulfanylation of alkynes using SF_5Cl in THF

The scope of the reaction was evaluated with previously utilized substrates as well as new ones, including aromatic and aliphatic and internal and terminal alkynes. The desired products were isolated in moderate to good yields and generally in better yields and with better selectivity than the previously utilized methods. For instance, the formation of the 2:1 adduct is minimized, while electron-withdrawing substituents on the aromatic ring are now tolerated.

Also in 2024, Wang and Qin performed the copper-initiated regiodivergent chloropentafluorosulfanylation of 1,3-enynes using SF_5Cl.[14] The regioselectivity was mainly related to the structure of the enyne. Indeed, substrates containing a terminal alkene were selectively converted into the corresponding SF_5-substituted propargylic chlorides **6** (Scheme 6). Whereas only the SF_5-substituted 1,3-dienes **7** were obtained in case of 4-unsubstituted 1,3-enynes. Moreover, access to allene **8** was possible for a 1,3-enyne containing bulkier substituents at the 2-position compared to that at the 4-position. The scope of the different reactions has been evaluated and demonstrated a remarkable tolerance with several substrates bearing different functional groups. Mechanistic experiments revealed again the radical pathway, which is initiated with the formation of $SF_5^{\bullet}$ radicals via SET between SF_5Cl and the Cu(I) complex.

The highly strained bicyclo[1.1.1]pentane (BCP) has recently emerged as a valuable pharmaceutical bioisostere of benzene rings, since the replacement of aryl substituents with 1,3-disubstituted BCP can improve passive permeability, aqueous solubility, and metabolic stability of drug candidates. Until 2022, access to C(sp^3)–SF_5 and C(sp^3)–SF_4Ar bonds was limited to the addition of SF_5 and Ar-SF_4 radicals to alkenes. In order to overcome this limitation, Cornella, Pitts, and co-workers developed a mild radical chloropenta-

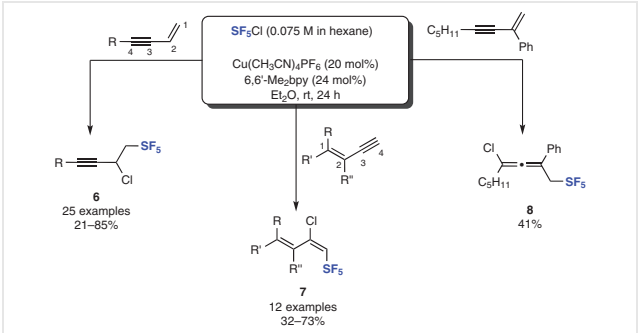

Scheme 6 Copper-initiated regiodivergent chloropentafluorosulfanylation of 1,3-enynes using SF_5Cl

fluorosulfanylation and tetrafluoro(aryl)sulfanylation of [1.1.1]propellane leading to the formation of new C(sp^3)–SF_5 and C(sp^3)–SF_4Ar bonds in the corresponding bicyclopentanes, these latter unusual species called 'hybrid isosteres' have been fully characterized and structurally analyzed.[15] This transformation uncovered the transannular C–C distance in SF_5-BCP-Cl as the shortest reported nonbonding C···C distance. Thus, first they investigated the generation of SF_5 radicals from SF_5Cl in the presence of [1.1.1]propellane (**9**) and white LEDs irradiation resulting in the desired volatile SF_5-BCP-Cl product **10** in 86% yield (Scheme 7). Mechanistic studies suggested that [1.1.1]propellane (**9**) is involved in the initiation step and that SF_5 radicals are formed, initially through visible light excitation of an electron donor-acceptor complex between SF_5Cl and **9**, that propagate a radical chain reaction. The SC-XRD of compounds **10** and **12** allowed measurement of the distance between C1···C3 (1.789 Å) and C1···C4 (2.745 Å). A similar average S–F_{eq} distances of roughly 1.57–1.59 Å for the equatorial fluorine (F_{eq}) atoms was observed on both **10** and **12**, while the $\theta_{C3\text{-}S\text{-}Feq}$ angle for both **10** and **12** deviates slightly from perpendicularity with ~92.3° and ~92.6°. The axial S–F_{ax} bond length in **10** (1.579 Å) and **12** (1.587 Å) are also in a similar range. DFT calculations along with literature supported the notion that donor-acceptor interactions involving the 'wing' C–C bonds in BCP rings play a significant role in this shortening phenomenon. Additionally, they investi-

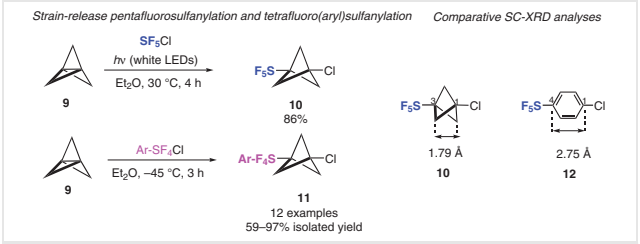

Scheme 7 Pentafluorosulfanylation and tetrafluoro(aryl)sulfanylation of [1.1.1]propellane

gated the reaction between Ar-SF_4Cl with **9** affording compound **11**. The reaction could occur in the absence of light as Ar-SF_4Cl and **9** could initiate the radical chain by themselves. The scope of accessible arene- and heteroarene-containing compounds was explored including pyridine- and pyrimidine-containing substrates.

In 2023, Qing and co-workers developed a one-pot iodopentafluorosulfanylation of [1.1.1]propellane (**9**) with SF_5Cl and CH_2I_2 for the practical synthesis of iodopentafluorosulfanylated bicyclo[1.1.1]pentane (SF_5-BCP-I, **13**) as an applicable platform to functionalized SF_5-BCP scaffolds.[16] As SF_5I cannot be synthesized and has never been detected (*vide supra*), this work used SF_5Cl in the presence of CH_2I_2 as an iodinating agent. Indeed, compound **13**, a bench stable and easy-handling solid, was obtainable as the major product in 73% yield on a gram scale (Scheme 8).

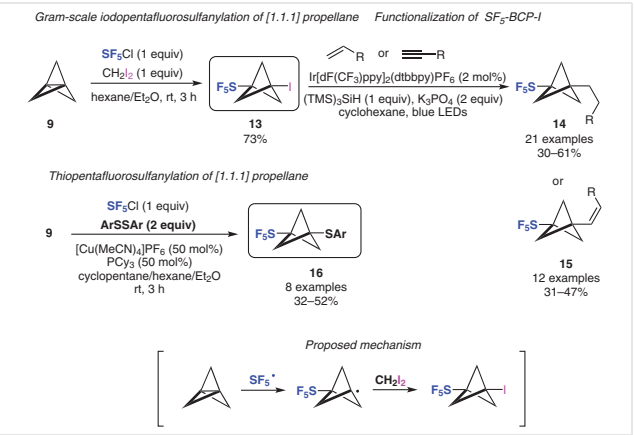

Scheme 8 Synthesis of iodopentafluorosulfanylated bicyclo[1.1.1]pentane (SF_5-BCP-I) and its functionalization

Mechanistic studies were conducted in order to understand the mechanism of the iodopentafluorosulfanylation reaction that revealed a radical chain propagation pathway initiated by the autoinitiation of SF_5Cl. The proposed mechanism is shown in Scheme 8; the $SF_5^{\bullet}$ radical adds to **9** to give the SF_5-BCP$^{\bullet}$ radical intermediate, which abstracts iodine atom from CH_2I_2 to furnish SF_5-BCP-I **13**.

SF_5-BCP-I **13** was further functionalized by an Ir-catalyzed, silane-mediated photoredox radical addition of alkenes. Using the optimized conditions, the scope of the reaction was investigated with a wide range of substituted styrenes, substituted alkenes, and various heteroaryl-substituted alkenes forming compounds **14** in moderate to good yields. Additionally, the reaction took place with alkynes leading exclusively to the corresponding *Z*-alkenes **15** in moderate yields. The preparation of SF_5-BCP-SR **16** was also investigated using diaryl disulfides and SF_5Cl in the presence of $[Cu(MeCN)_4]PF_6$ and PCy_3. The scope of the thiopentafluorosulfanylation, occurring through a copper-promoted radical trapping process, was explored with various aryl rings.

Similar to BCPs, cyclobutane (CB) rings are being employed more frequently in medicinal chemistry, e.g., as bioisosteric replacements for arenes or alkenes. In contrast to SF_5-BCPs, the non-linear exit vectors of SF_5-CBs afford an added degree of flexibility in the three-dimensional organization of the SF_5 group. In 2024, the Pitts group reported the strain-release functionalization of bicyclo[1.1.0]butanes (BCBs) **17** using SF_5Cl.[17] These methods allowed the preparation of the first SF_5-containing cyclobutanes with 1,3-substitution patterns. Pentafluorosulfanylation of a variety of sulfone-substituted BCBs **17** in the presence of SF_5Cl under irradiation overnight with white LEDs gave SF_5-CB-Cl products **18** with polarity mismatch (Scheme 9, Method A (Met-A)). The *anti*/*syn* ratios observed using Method A range from 1:1 to 2.5:1, which is typical for radical addition reactions to similarly substituted BCBs. Notably, the isomers could be separated by chromatography. Then, the one-pot hydropentafluorosulfanylation of the same sulfone-substituted BCBs **17** under conditions of Method A but in the presence of $NaBH_4$ as reductant gave SF_5-CB-SO_2R **19** (Scheme 9, Method B (Met-B)). The *cis*/*trans* ratios observed using Method B range from 1:1 to 1.6:1 and often differ from ratios observed using Method A, suggesting that epimerization occurs during C–Cl bond reduction; this hypothesis was further confirmed by mechanistic study.

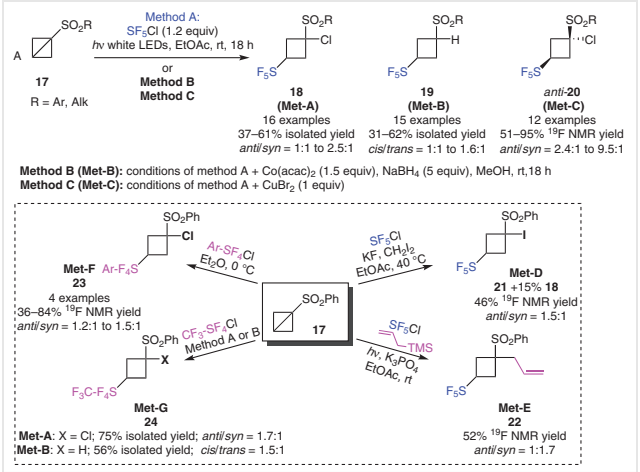

Scheme 9 The strain-release functionalization of bicyclo[1.1.0]butanes (BCBs) using SF_5Cl

Remarkably, the use of a transition metal salt such as $CuBr_2$ resulted in an *anti*-stereoselective variant of Method A, in which the *anti*-isomer **20** was favorably formed in good yields, with *anti*/*syn* ratios ranging from 2.4:1 to 9.5:1 (Scheme 9, Method C (Met-C)). This method represents a rare case in which a transition metal additive overrides substituent influence on selectivity of the radical addition on BCBs.

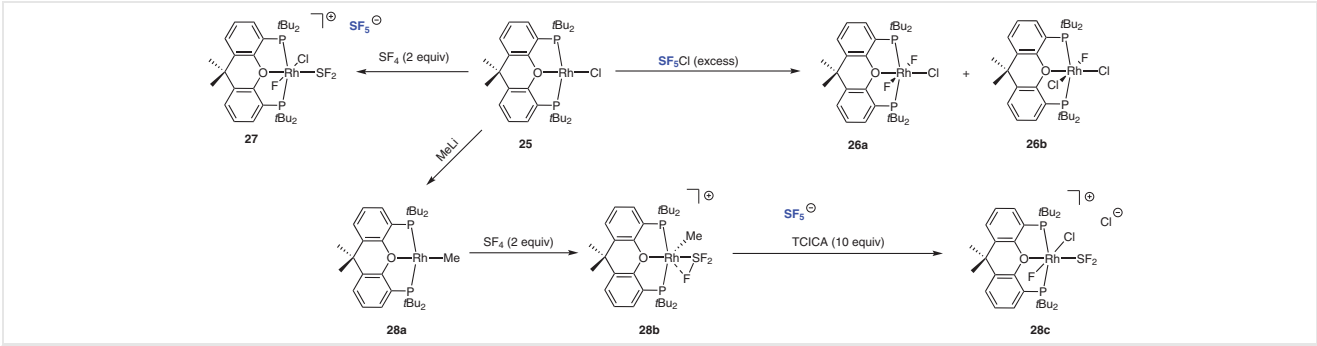

Scheme 10 The use of SF_5Cl for the preparation of Xantphos-type Rh complexes

Moreover, the iodopentafluorosulfanylation, pentafluorosulfanylation-allylation, tetrafluoro(aryl)sulfanylation, and tetrafluoro(trifluoromethyl)sulfanylation of 1-(phenylsulfonyl)bicyclo[1.1.0]butane (**17**, R = Ph) were investigated and allowed the preparation of the corresponding products **21**, **22**, **23**, and **24** in good yields (Scheme 9, Methods D–G (Met-D, Met-E, Met-F, Met-G)). Other electron-withdrawing groups instead of sulfone were investigated in order to play on the polarity mismatch. Thus, BCB with ketone, ester, amide, nitrile, halide, and boron-based groups were used. Again, the mismatched products were preferentially obtained. Nevertheless, in this case, the matched products could be observed in the reaction mixture as minor products. Mechanistic studies and DFT calculations have been conducted suggesting that chloropentafluorosulfanylation proceeds through an intriguing polarity mismatch addition of electrophilic SF_5 radicals to the electrophilic sites of the BCBs.

Beside its prominent role in the formation of the C–SF_5 bond by radical addition to unsaturated compounds, SF_5Cl was also utilized in the preparation of SF_3 generation of Xantphos-type Rh complexes.[18] Treatment of complex **25** with excess SF_5Cl leads to the preparation of **26a** and **26b** in 0.2:1 ratio. These side products are obtained alongside the cationic complex **27** containing an SF_5 counterion in the reaction between **25** with 2 equivalents of SF_4. In this work, Braun and co-workers reported the full characterization of the obtained complexes including ^{19}F and ^{31}P NMR and single X-ray crystallography. Remarkably, oxidative chlorination of **28b** with trichloroisocyanuric acid (TCICA) results in chlorination of the SF_5 anion and the anionic methyl group, along with the formation of a Rh–Cl complex with a chloride counteranion (Scheme 10).

2.1.1 Generation of SF_5Cl

The use of SF_5Cl is a prominent approaches for the preparation of SF_5-containing compounds. SF_5Cl gas is commercially available in small gas cylinders or prepared in hexane stock solution from flowers of sulfur;[10,19] it requires safe handling and is still relatively expensive (25–30€ per gram). Indeed, there is urgent need to develop simpler, safer, and cheaper access to SF_5Cl.

De Borggraeve and co-workers focused on the development of an efficient strategy for on-demand SF_5Cl gas generation from 4,4′-dipyridyl disulfide, a commercial reagent.[20] The *ex situ* generation of SF_5Cl was successfully achieved in the presence of TCICA as chlorine source and KF in acetonitrile at room temperature. Performing this method in a two-chamber reactor allowed the direct applicability of the generated SF_5Cl in different known transformations with solvent flexibility. Thus, in the second chamber the radical addition of SF_5Cl (generated in the first chamber) to alkynes, alkenes, and 2-diazo-1-phenylethan-1-one was examined and afforded a limited scope of products with moderate to good yields (Scheme 11). Despite scaling this method up to 1 gram, it remains applicable only on a lab-scale. ^1H-^{19}F HOESY experiments performed on two different substrates confirmed the *E*-stereochemistry of the chloropentafluorosulfanylated alkenes from the reaction of SF_5Cl and alkynes. The mechanistic study suggests a possible concerted S_NAr between pyridine-SF_4Cl and fluoride to form fluoropyridine with the release of SF_5Cl.

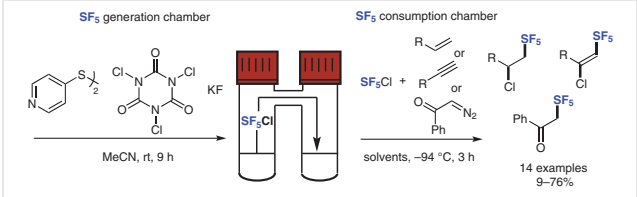

Scheme 11 Two-chamber SF_5Cl gas generation from 4,4′-dipyridyl disulfide in the presence of TCICA and KF

Sulfur hexafluoride (SF_6) is a nontoxic and inexpensive gas (~1€ per gram) with unique physical and chemical properties. Despite these advantages, it is one of the most potent greenhouse gases with a long lifetime of 3200 years in the atmosphere; these and other facts make the replacement of this gas and its degradation an essential challenge. In this context, Tlili and co-workers reported a metal-free activation of SF_6 under blue LED irradiation, leading to the

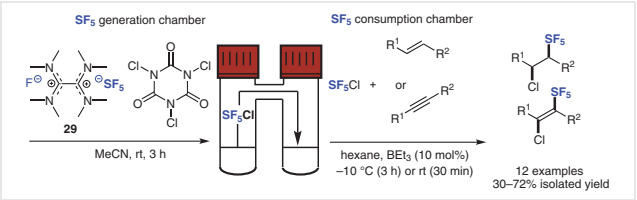

Scheme 12 Two-chamber SF_5Cl gas generation from reagent **29** in the presence of TCICA

preparation of an SF_5-based reagent used efficiently for the deoxyfluorination of CO_2, the fluorinative desulfurization of CS_2, and more interestingly for the *in situ* generation of SF_5-Cl ready for the pentafluorosulfanylation reactions of alkynes.[21] The activation of SF_6 took place in the presence of an organic electron-donor, tetrakis(dimethylamino)ethylene (TDAE), using blue LED light. Mechanistic studies relying on EPR spectroscopy, NMR, and cyclic voltammetry confirmed the formation of the ion pair reagent **29** under mild conditions. Thus, using a two-chamber reactor, **29** reacts with TCICA in MeCN to generate SF_5Cl, which was condensed in hexane in chamber 2 (Scheme 12). After several optimization trials, the pentafluorosulfanylation of different alkynes and alkenes was performed to give chloro-pentafluorosulfanyl-substituted alkanes and alkenes in good to moderate yields, by means of the *in situ* generated SF_5Cl in the presence of catalytic amount of Et_3B.

2.2 By Means of Oxidative Fluorination

Despite all the advantages of aromatic SF_5 molecules, their widespread application is hampered by the limited and low-yielding available synthetic methodology. Access to Ar-SF_5 compounds was achieved first by Sheppard in 1960 by the fluorination of diaryl disulfides with AgF_2 resulting in low yields and chemoselectivity.[3c] Recent approaches introduced by Umemoto,[22a] Togni,[22b] Shibata,[22c] and Cornella[22d,e] involved a stepwise oxidative fluorination sequence of diaryl disulfides into arylsulfur chlorotetrafluoride Ar-SF_4Cl as intermediate which undergoes a Cl–F exchange (Scheme 13).[6]

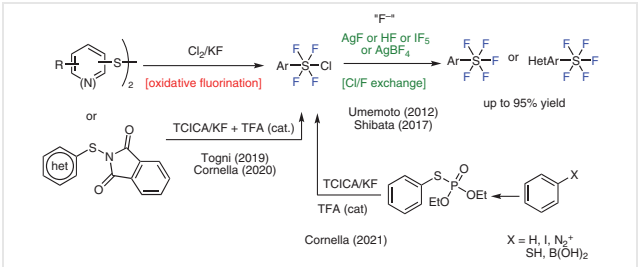

Scheme 13 Recent approaches for oxidative fluorination to access aromatic SF_5 molecules

However, some limitations remain associated with these methods such as multistep sequence, moderate yields, limited functional group tolerance, highly sensitive handling of Ar-SF_4Cl intermediates, and limited set of available starting materials. Based on this, in 2023 Gatzenmeier and Nozaki reported (in a preprint) a revised version of the Sheppard conditions for the oxidative pentafluorination of thiophenol derivatives to obtain Ar-SF_5 in good yields.[23] It was shown that the use of two equivalents NEt_4Cl in the presence of an excess of AgF_2 in MeCN for less than 1 hour efficiently gave pentafluorosulfanyl-substituted arenes **30** in up to quantitative yield (Scheme 14). Similar efficiency has been obtained by using other onium salts such as Bu_4NCl, Et_4NBr, and Ph_4PX (X = F, Cl, and Br). Interestingly,

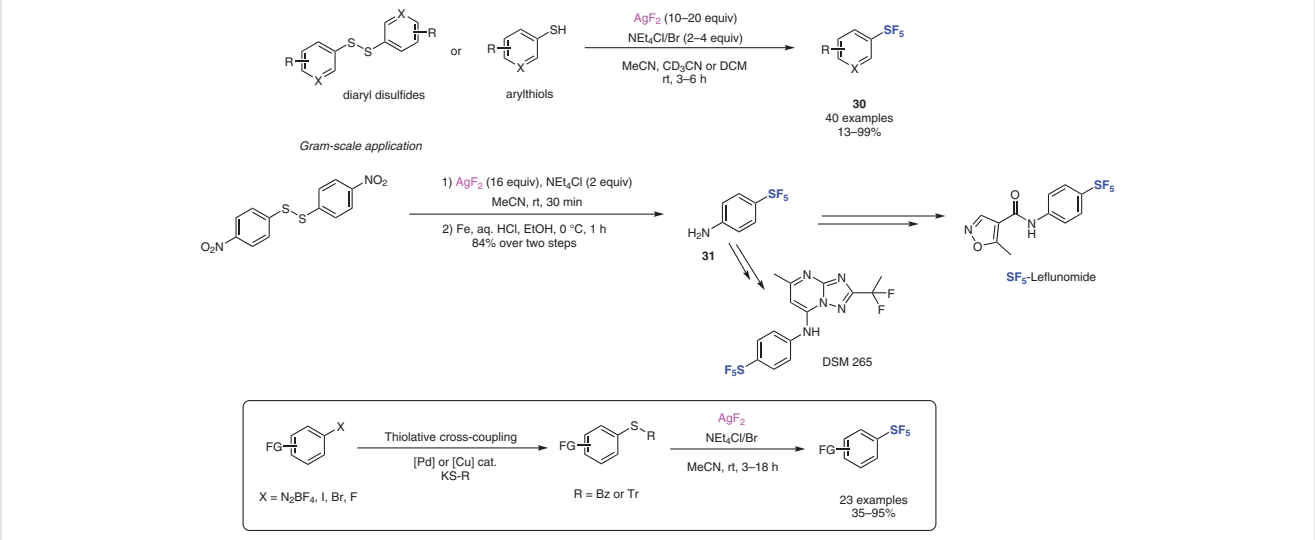

Scheme 14 Oxidative pentafluorination of thiophenol derivatives using AgF_2

no other products except for traces (<2%) of hydrolyzed sulfur compounds (Ph-SO_2F, PhSOF) were detected. The silver(I) byproducts (AgF, AgCl) can easily be filtered off and could be fluorinated back to AgF_2 with industrial F_2 gas. Furthermore, the substrate scope for both diaryl disulfide and arenethiols was investigated demonstrating the high applicability of this methodology; the scope was extended to 40 molecules with different substituents and functional groups without including substrates bearing electron-donating substituents. Gram-scale oxidative fluorination was carried out on a 4-mmol scale for the synthesis of compound **31**, which is an intermediate for the synthesis of SF_5-leflunomide, displaying twofold greater potency than its original, commercialized CF_3-version, and the antimalarial drug DSM265, the first SF_5-compound in clinical development.

The oxidative fluorination of thiobenzoates and trityl sulfides proceeded smoothly in the presence of some functional groups as well as oxygen- or nitrogen-containing heterocycles in good to excellent yields.

De Borggraeve and Ismalaj reported a gas-cylinder-free and glovebox-free strategy to access S(IV) and S(VI) fluorinated compounds.[24] Using a two-chamber reactor, the team used calcium hypochlorite ($Ca(OCl)_2$, CLOgen) in combination with sulfuric acid in the first chamber to *ex situ* generate chorine gas which is dissolved in the second chamber containing KF along with aliphatic or (hetero)aromatic thiols. The oxidative halogenation carried out under these conditions allowed, depending on the quantity of H_2SO_4 and the quality of reagents, the preparation of Ar-SF_4Cl, Ar-SO_2F, and Ar-SF_3 compounds in good to excellent yields (Scheme 15). Compounds Ar-SO_2F were mainly formed due to the hydrolysis of Ar-SF_4Cl, while Ar-SF_3 compounds are obtained when less $Ca(OCl)_2$ is used. The scope of the reactions was evaluated in each case enabling access to a large library of the desired products. Moreover, the post-functionalization of Ar-SF_4Cl compounds was performed to access SF_4-bridged indole, α-SF_4-Ar ketones, and, interestingly, the corresponding SF_5 analogues.

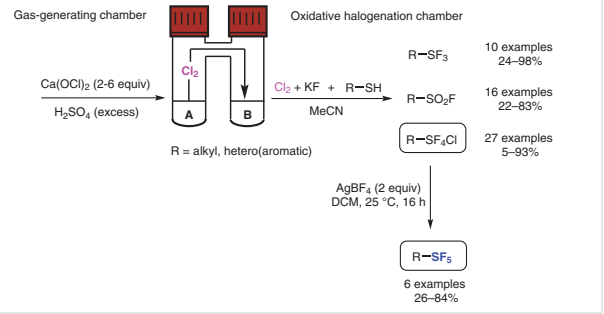

Scheme 15 A gas-cylinder-free strategy to access S(IV) and S(VI) fluorinated compounds

2.3 By Means of SF_5-Alkynes

Nowadays, SF_5-alkynes are easily accessible and versatile substrates.[25] Our group and others work actively to broaden the substrate scope and unlock new reactivities.

In 2024, the Paquin group developed a 1,3-dipolar cycloaddition of diazoacetate **33** with SF_5-alkynes **32** to access to 3- and 4-SF_5-pyrazoles **34** and **35**.[26] They performed this transformation using a flow reactor to minimize the concentration of diazoacetate, which is potentially explosive when used in batch. Even if a mixture of these two isomers **34** and **35** is obtained in all the cases whatever the substitution of **33**, they observed a slight inversion of selectivity when the SF_5-alkynes **32** is substituted with an aryl or an alkyl chain (Scheme 16).

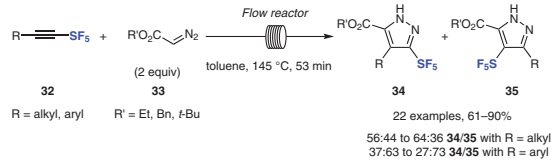

Scheme 16 1,3-Dipolar cycloaddition of diazoacetate with SF_5-alkynes to access to 3- and 4-SF_5-pyrazoles under flow conditions

The same year, the Bizet group reported a fully regioselective synthesis of 2-SF_5-inden-1-ol **38** (X = O) and -inden-1-amine **38** (X = NH) catalyzed by a palladium complex. The reaction proceeds smoothly starting from aromatic and aliphatic SF_5-alkynes and can be performed either with boronic acids, esters, or trifluoroborate salts. The 2-SF_5-inden-1-ols **38** (X = O) were further oxidized to 2-SF_5-indenones **39** in the presence of manganese oxide, and these compounds proved to be competent Michael acceptors with N- and S-nucleophiles delivering the corresponding products **40** in high yields with predominantly *anti*-configuration (Scheme 17).

The SF_5 group is an electron-withdrawing motif that polarizes the C≡C bond of alkynes. In 2023, the Bizet group took advantage of this polarization to develop regio- and

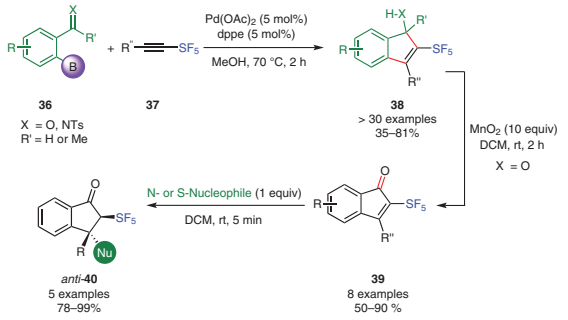

Scheme 17 Palladium-catalyzed regioselective synthesis of 2-SF_5-inden-1-ols and further derivatizations

stereoselective hydroelementation reactions of SF_5-alkynes.[27] They reaction was compatible with a wide range of N-, O- and S-nucleophiles, which were added exclusively to Cβ and yielded in all the cases the β,*Z*-product **41**. Given that the reaction is performed under basic conditions, it was possible to engage directly the SF_5-chloro-alkene with the nucleophile, in the presence of base giving the same selectivity and yields for **41** regardless of the nature of the nucleophile. This methodology was successfully extended to piperidine or pyrrolidine as the nucleophile followed by an acidic workup to develop an easy and rapid access to α-SF_5 ketones **43** (Scheme 18).

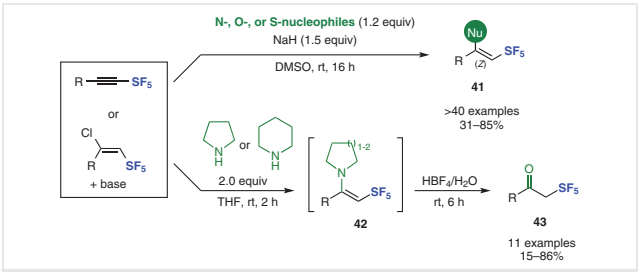

Scheme 18 Regio- and stereoselective hydroelementation of SF_5-alkynes and further functionalizations

The origin of the selectivity was explained by DFT calculations. The natural charges from a Natural Population Analysis (NPA) of the SF_5-alkyne was calculated to be +0.09 for Cβ and –0.030 for Cα (with R = *p*-Ph-C_6H_4) which means that Cβ is slightly electrophilic which make it a privileged site for nucleophilic attack.

The β-selectivity was confirmed by a larger steric repulsion (ΔE_{Pauli}) upon the attack at Cα and the *Z*-isomer seemed to be kinetically favored ($\Delta G^{\ddagger}$ = 21.7 kcal/mol) compared to the *E*-isomer ($\Delta\Delta G^{\ddagger} \approx 5$ kcal/mol). Simultaneously, similar reactivity was observed by the Rombach group by performing the hydroamination reaction with TIPS-SF_5-acetylene **44** as single substrate.[28] The procedure they developed involves the deprotection of the silyl moiety with formation

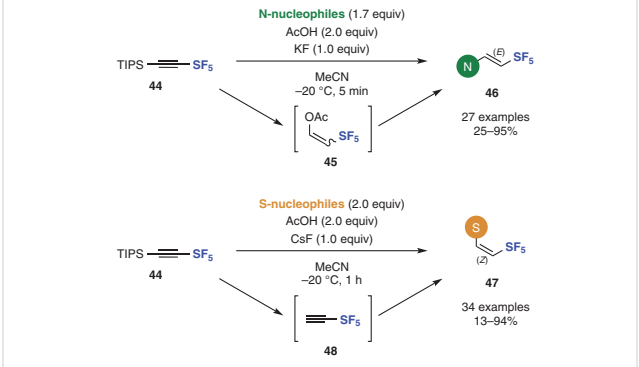

Scheme 19 Stereoselective hydroamination and hydrothiolation of TIPS-SF_5-acetylene

of several intermediates, including enol acetate **45**, all leading to the formation of the β,*E*-enamines **46** in the presence of N-nucleophiles (Scheme 19). A detailed DFT calculation study was performed but a very small difference in transition state Gibbs free energies was calculated for the direct *E*/*Z*-nucleophilic addition of the amine onto SF_5-acetylene ($\Delta\Delta G^{\ddagger} \approx 0.3$ kcal/mol in favor of the *Z*-isomer). Several mechanistic pathways were proposed with the formation of β,*E*-enamines **46** as the thermodynamically more stable product.

Similarly, they developed hydrothiolation of TIPS-SF_5-acetylene **44** under similar reaction conditions; the β,*Z*-vinyl sulfide **47** was obtained as single stereoisomer.[29] The enol acetate **45** proved not to be a productive intermediate in this transformation, which seemed to proceed through a direct nucleophilic attack of the thiol on to the SF_5-acetylene **48** leading to the kinetically favored β,*Z*-product **47** ($\Delta G^{\ddagger}$ = 13.9 kcal/mol with a $\Delta\Delta G^{\ddagger} \approx 5$ kcal/mol).

Along with the same concept, in 2024 the Shibata group developed a regio- and stereoselective hydrofluorination reaction of RSF_4- and SF_5-alkynes **49** using tetrabutylammonium fluoride (TBAF·3H_2O) as fluoride source delivering exclusively the β,*Z*-fluoro-alkene **51** in moderate to good yields (Scheme 20).[30] DFT calculations confirmed that β,*Z*-intermediate **50** is formed faster than the β,*E*-isomer ($\Delta G^{\ddagger}$ = 15.3 kcal/mol for the β,*Z*-isomer vs $\Delta G^{\ddagger}$ = 19.0 kcal/mol for the β,*E*-isomer). The reaction proceeds through the nucleophilic addition of a fluoride anion to the electropositive Cβ, while the carbanion at Cα is quickly protonated by the water contained in TBAF. The reaction proved to be very efficient with aryl- and heteroaryl-substituted alkynes while a complex mixture was obtained with aliphatic substrates.

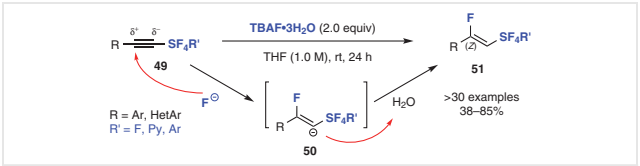

Scheme 20 Regio- and stereoselective hydrofluorination reaction of RSF_4- and SF_5-alkynes

Simultaneously and independently, Bizet, Cahard, Miqueu, and co-workers reported the same year the regioselective and stereodivergent hydrohalogenation of SF_5-alkynes with all the halogens (I, Br, Cl, F).[31] Once again, the regioselectivity is controlled thanks to the polarization of the SF_5-alkyne with selective introduction of halides on the electro-positive Cβ.

In this case, both *E*- and *Z*-stereoisomers were obtained selectively and separately following two distinct reaction mechanisms: The first one relies on the use of halides and a weak acid (AcOH) where a nucleophilic addition of the halide (I, Br, Cl) takes place on the Cβ, followed by the reprotonation of the intermediate anion **52** with the acetic acid delivering selectively the β,*Z*-SF_5-halo-alkene **53** (Scheme

21a). In the second mechanism, the alkyne plays the role of the nucleophile and is first protonated with a strong acid (HI or TFA); the intermediate carbocation **54** reacts then with the halide on the most accessible face (opposite side to SF_5 due to bulk) to generate the β,*E*-SF_5-halo-alkene **55** (Scheme 21b).

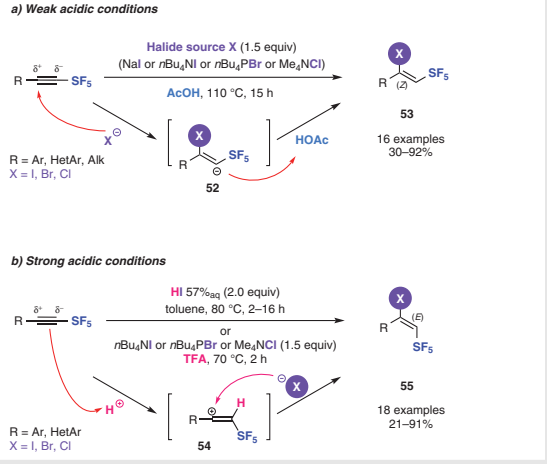

Scheme 21 Regioselective and stereodivergent hydrohalogenation of SF_5-alkynes with all the halogens

With the help of the EDA method, it was shown that the stronger interaction between the reactants upon the formation of *E*-alkenyl halides is due to a smaller overlap between the main occupied orbitals of the reactants, ultimately leading to lower Pauli repulsion. Stereodivergent fluorination has been also studied and a same reactivity as the Shibata group[30] was obtained using TBAF solution resulting in β,*Z*-**55** in 69% yield (Scheme 22a); the use of an acid additive was detrimental in this case. On the other hand, using an excess of 2,6-dichloropyridinium tetrafluoroborate in DCE at 80 °C allowed the formation of the opposite β,*E*-SF_5-fluoro-alkene **56** (90:10 *E*/*Z* **56**/**55** selectivity) in 51% isolated yield (Scheme 22b).

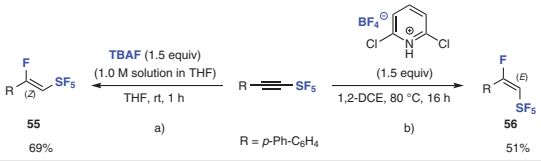

Scheme 22 Stereodivergent fluorination of SF_5-alkynes

Taking advantage of this dual reactivity SF_5-alkyne as both an electrophile and a nucleophile, regio- and stereoselective dihalogenation of SF_5-alkynes was developed with I_2, ICl, and Br_2. The *Z*-dihalogenated alkenes **57** are formed as major products whatever the nature of the halogens (Scheme 23a).[31]

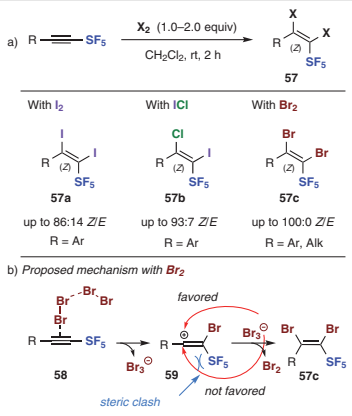

Scheme 23 Regio- and stereoselective dihalogenation of SF_5-alkynes with I_2, ICl, and Br_2

Noteworthy, with ICl, the iodine atom is selectively introduced at Cα and the chlorine atom at Cβ. The mechanism of the dibromination was also investigated by DFT calculations confirming that the reaction pathway involves the formation of a bromo-vinyl cation **59** rather than a bromonium cation, followed by the addition of Br^-, from Br_3^-, the opposite side to that of SF_5 mainly because it induces a strong steric repulsion (Scheme 23b).

2.4 Other Miscellaneous Aromatic and Aliphatic SF_5-Compounds

The SF_5 group shows surprising levels of chemical and thermal stability and especially compared to other S–F compounds that could be easily substituted. In 2023, the Breher group and the Paradies group demonstrated that aromatic-SF_5 can be converted into thiols, silyl-protected thiols, and diaryl sulfides in high yields (25–93%).[32] These transformations can occur thanks to a catalytic amount of

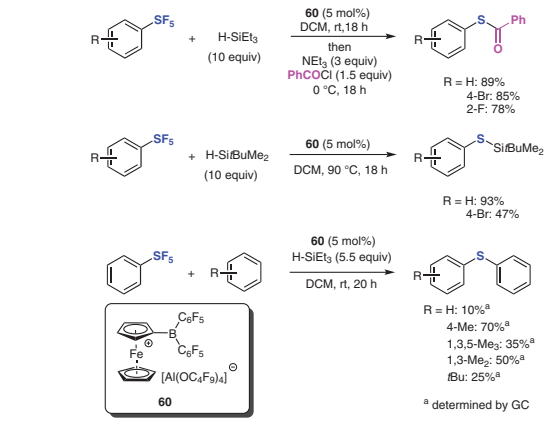

Scheme 24 Defluoro-functionalization of SF_5-arenes via activation of a S–F bond by a boron-centered Lewis superacid

boron-centered Lewis superacid 60. This diaryl ferrocenium borane can activate the S–F bond as well as the C–F bond (Scheme 24).

Moreover, SF_5-arenes could be functionalized in the *ortho* position via lithiation reactions, under strictly controlled conditions (Scheme 25).[33] Daugulis and Le reported the *ortho*-lithiation of diverse SF_5-arenes with lithium tetramethylpiperidide (5 equiv.) in THF/pentane at –60 °C; Barbier conditions were crucial to the success of the electrophilic trapping. Different classes of electrophiles are competent, such as chlorosilanes, chlorogermanes, or ditin derivatives. The reaction is general (18 examples) and gives 2-substituted SF_5-arenes **61** in good yields (50–95%). In specific cases, it was observed that the *ortho*-directing effect of SF_5 was less efficient than the one imparted by a nitrile or a methoxy (not shown). In addition, SF_5 could act as a leaving group above –40 °C leading to the corresponding aryne **62** that in turn could be trapped by lithium tetramethylpiperidide leading to a 1:1 mixture of **63** and **64**.

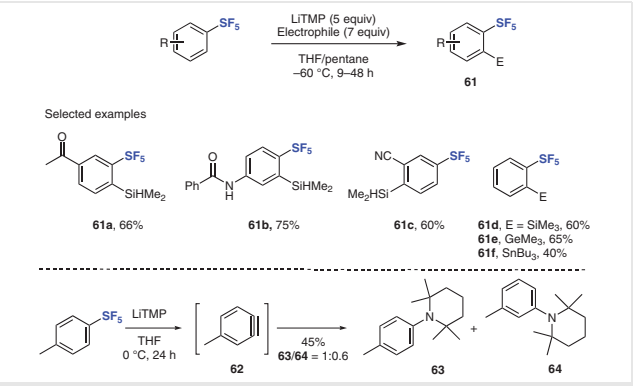

Scheme 25 In situ *ortho*-lithiation/functionalization of SF_5-arenes

Along with the functionalization of SF_5-arenes, Michaut and co-workers from Novalix reported, in 2021, the synthesis of functionalized *m*-SF_5-phenols and their use as building blocks for the synthesis of 2-arylindanediones.[34] These latter compounds possess vitamin K antagonist activity. Several sequential reactions on the commercially available SF_5-phenol have been performed in this work (Scheme 26). Indeed, they prepared a wide range of SF_5-anisoles bearing diverse substitutions such as ester, aldehyde, halogens, alcohol, nitrile, and carboxylic acid with good to excellent yields. These compounds have potential as high-value building blocks for the synthesis of various scaffolds. Finally, they performed the condensation of anisoles **66** and **69** with commercial phthalide or 4-nitrophthalic anhydride, respectively, followed by downstream functionalization to increase molecular complexity to obtain 2-arylindanediones **68** and **70**. This collection of SF_5-substituted 2-arylindanediones has the potential to be included in medicinally relevant compound libraries.

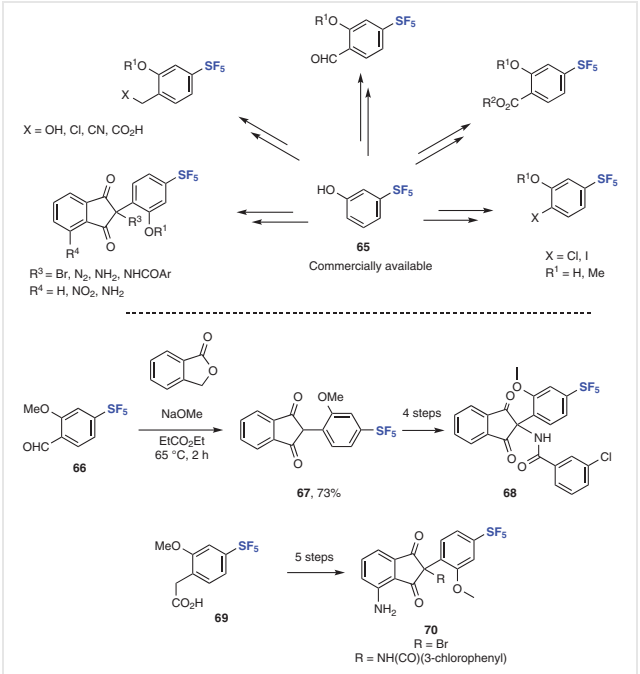

Scheme 26 Synthesis of substituted *m*-SF_5-phenols and their use in the synthesis of 2-arylindanediones

In 2023, Lam, Paquin, and Mastalerz extended the Kolbe electrolysis reaction to access aliphatic SF_5-compounds. In this electrochemical approach 2-(pentafluorosulfanyl)acetic acid is reacted with an aliphatic carboxylic acid.[35] The reaction proceeded in low to moderate NMR yield and was extended to 9 examples including primary aliphatic, benzylic, and secondary aliphatic derivatives (Scheme 27).

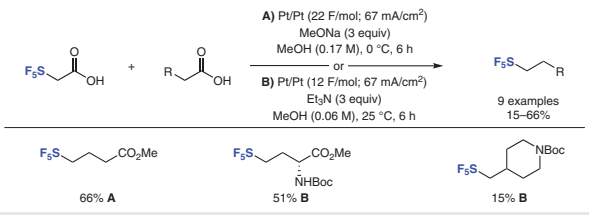

Scheme 27 The synthesis of aliphatic SF_5-containing compounds using the Kolbe reaction

Also in 2023, Paquin, Charette, and co-workers developed a rhodium-catalyzed intramolecular cyclopropanation of 3-(pentafluorosulfanyl)allyl cyanodiazoacetates.[36] This sequence gave access not only to 5 examples of cyclopropane-fused γ-lactones **71** in moderate yields (55–66%), but also to highly functionalized SF_5-substituted cyclopropanes. In addition, an asymmetric version of this reaction was attempted for the first time using Rh_2(s-nap)$_4$ as a catalyst; a modest 8% yield was obtained but with promising 66% ee that suggests enantioselective version of the reac-

tion will soon be developed. In addition, these scaffolds can be further used to access highly functionalized SF_5-substituted cyclopropanes. For example, the treatment with benzylamine in the presence of LiCl gave a tetrasubstituted cyclopropane in high 86% yield (Scheme 28).

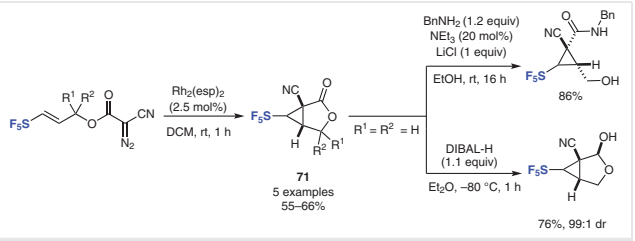

Scheme 28 Rhodium-catalyzed intramolecular cyclopropanation of 3-(pentafluorosulfanyl)allyl cyanodiazoacetates

The synthesis and reactivity of difluoroiodo(pentafluorosulfanyl)methane (**74**) was explored by Haufe and coworkers (Scheme 29).[37] This reagent, prepared in two steps from difluoro(pentafluorosulfanyl)acetic acid (**72**) under Hundsdiecker conditions, can generate the corresponding electron-deficient radical in the presence of triethylborane. This radical can add to electron-rich π-systems as in the case of butyl vinyl ether (**75**). However, electron-rich aromatics such as trimethoxybenzene lead to a different reactivity as only difluoromethylenation is observed. The difluoro(pentafluorosulfanyl)methylene radical can also add to strained alkenes, such as in the case of cyclooctadiene **77**; a transannular cyclization occurs delivering the bicyclo derivative **78** in 41% yield. Alkyl-substituted alkenes **79** can also be engaged in this radical difluoro(pentafluorosulfanyl)methylenation, leading to moderate to good yields of the corresponding linear derivatives **80**, which are sensitive to various downstream functionalizations. As could be anticipated based on the polarity of the reactive species, electron-deficient alkenes such as cyclohexenone are unreactive.

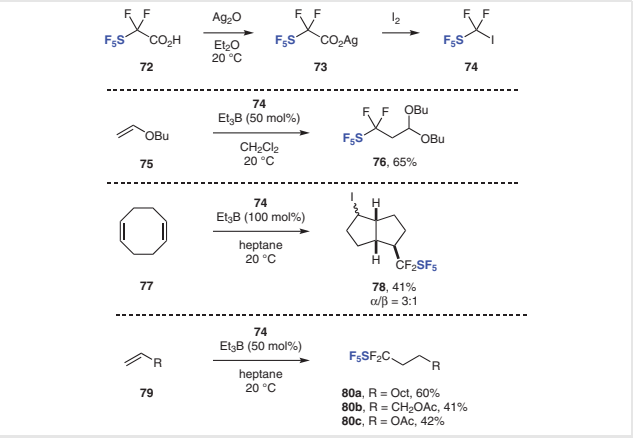

Scheme 29 Reactions of difluoroiodo(pentafluorosulfanyl)methane (SF_5CF_2I) with electronically different types of alkenes

3 Applications

3.1 Medicinal and Biological Chemistry

The introduction of a SF_5 substituent to organic molecules leads to important changes enhancing different parameters such as stability, bulkiness, and lipophilicity. This makes the SF_5 group a first-class substituent for next generation drug discovery. In 2022, Sani and Zanda reviewed different applications of molecules bearing SF_5.[6a] Herein, we will report published reports during last three years.

Curcumin has previously shown promising effects in the treatment of pancreatic cancer, which is a disease with high mortality risk. However, curcumin suffers from inadequate efficacy and bioavailability, preventing its clinical approval. In 2023, the Biersack group developed a series of synthetic curcuminoids and compared their activity to curcumin against various cancer types.[38] High activity was observed with mono-, di-, and trifluoromethyl derivatives, whereas SF_5 derivatives **82** appeared to be less active for the antiproliferative activity against human MiaPaCa-2 (IC_{50} = 2.48 μM for SF_5 vs 0.32 μM for CF_3) and Panc-1 pancreatic carcinoma cells (IC_{50} = 3.78 μM for SF_5 vs 0.77 μM for CF_3). In this case the trifluoromethyl substituent was superior to the pentafluorosulfanyl substituent regarding antiproliferative activity against pancreatic cancer cells (Figure 1a). Also in 2023, in order to improve the activity of curcuminoid derivatives, they developed a new (semi)synthetic curcuminoid derivative MePip-SF_5 **84** and they investigated its antitumor effects in a preclinical model of pulmonary melanoma metastasis.[39] MePip-SF_5 **84** was almost five times more effective in inhibiting B16F10 melanoma cell proliferation than its original substance of curcumin (IC_{50} MePip-SF_5 2.8 vs. 13.8 μM) and showing no *in vivo* toxicity up to 60 mg/kg (Figure 1b). MePip-SF_5 **84** was then tested in murine pul-

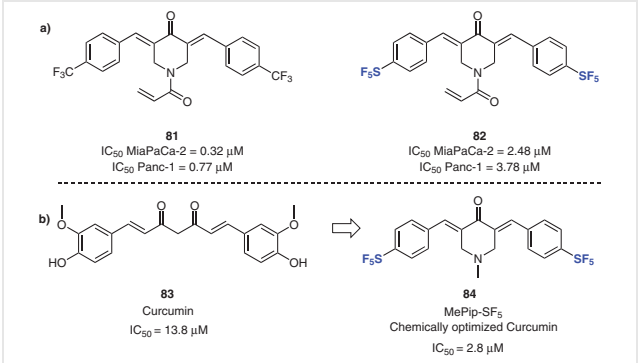

Figure 1 Curcumin and its derivatives

monary metastatic melanoma and showed a significantly lower pulmonary macroscopic and microscopic tumor load than the vehicle-treated controls. This novel curcuminoid MePip-SF_5 **84** showed a convincing antimetastatic effect and a lack of systemic toxicity in a relevant preclinical model of metastasized melanoma.

Cancer is a complex disease and is adaptive in such a way that it can promote proliferation and invasion thanks to an overactive cell cycle and, in turn, cellular division. This can be targeted by antimitotic drugs that are highly validated chemotherapy agents. In 2022, the Tillekeratne group reported a new class of imidazole-based chalcones as potential antimitotic agents.[40] Thanks to promising cytotoxic activity, a comprehensive structure-activity relationship (SAR) was carried out. *In silico* studies demonstrated that the series have the ability to bind to the colchicine binding site of β-tubulin. This tubulin binding can partially explain the biological effects. Even if the lead compound IBC-2 **85** is the on-going target for further investigation of its biological targets, SF_5-derivative IBC-24 **86** displayed good cytotoxic to cancer cells in the low micromolar range. IBC-24 **86** was evaluated in the NCI-60 human tumor cell lines screen, including leukemia, CNS cancer, ovarian cancer, or colon cancer, for example (Figure 2). The heat map of the mean proliferation values using data obtained from NCI-60 one dose assay showed that IBC-24 **86** was one of the more active.

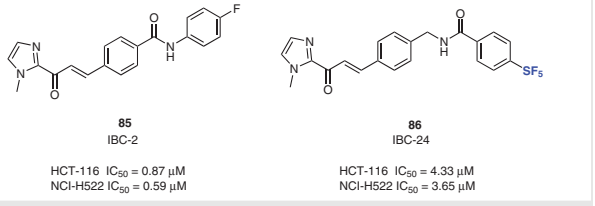

Figure 2 Activity of SF_5 imidazole-based chalcone

Conceptually, in cancer immunotherapy, the body's immune system attacks and eliminates a cancerous tumor. Among the approaches developed, some are based on the inhibition of the CD73 enzyme. The ability to potently inhibit CD73 using pyrimidine-based nucleotide analogues provides new opportunities for translational studies for cancer treatment. In this optic in 2022, the Jacobson group reported N^4-substituted 3-methylcytidine-5′-α,β-methylenediphosphates as CD73 inhibitors and investigated the structure-activity relationship.[41] The most potent analogue **87** contained 4-iodo substitution of the N^4-benzyloxy group with a K_i value of 0.436 nM, which represents a 10–20-fold increase in potency compared to the previously most potent inhibitors in this series. However, the SF_5-analogue **88**, which is both highly electron-withdrawing and strongly lipophilic, provided a K_i of 0.511 nM and appeared to be the third best hit of the series just behind the bromo derivative (Figure 3).

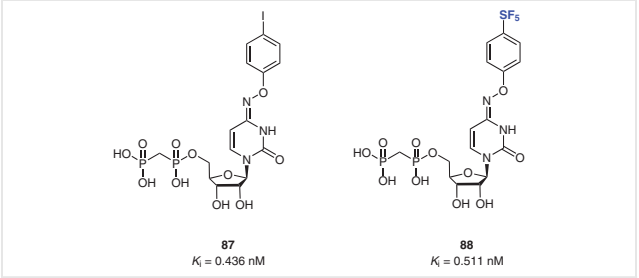

Figure 3 N^4-Substituted 3-methylcytidine-5′-α,β-methylenediphosphate derivatives as CD73 inhibitors

Dihydroorotate dehydrogenase (DHODH) catalyzes a key step in pyrimidine biosynthesis and has been recently validated as a therapeutic target for malaria. In 2022, Williams, Phillips, and co-workers proposed the use of dihydroorotate (DHO), an upstream metabolite of DHODH, as biomarker of DHODH inhibition.[42] It appeared that the treatment of mammalian cells with DSM265 **89** led to increases in DHO where the extent of biomarker buildup correlated with both dose and inhibitor potency on DHODH. It was found that DSM265 **89** selectively inhibits *Plasmodium* DHODH over the human enzyme. DSM 265 **89** display much higher activities than leflunomide **91** (Arava®) or its active metabolite Teriflunomide **90** (Aubagio®) and at the same time a lower toxicity (Figure 4). DSM 265 **89** is the only DHODH inhibitor drug candidate to reach clinical development for malaria showing good safety and efficacy for both treatment and prevention of *Plasmodium falciparum* malaria, including demonstrating a single dose cure of patients with *P. falciparum* malaria in trials in Peru.

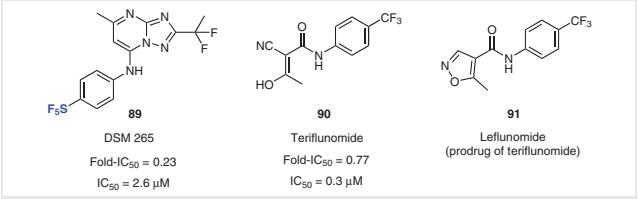

Figure 4 Clinically used DHODH inhibitors

Since the pentafluorosulfanyl (-SF_5) functional group is of growing interest as a bioisostere in medicinal chemistry, the Spencer group support by the Covid Moonshot Consortium synthetized, in 2022, a library of SF_5-containing compounds, including amide, isoxazole, and oxindole derivatives to expand the repertoire of low-molecular-weight SF_5-scaffolds.[43] All compounds were tested against targets including human dihydroorotate dehydrogenase (HDHODH) but none had any appreciable enzyme activity. A subsequent approach led to synthesis of analogues of the clinically used disease modifying anti-rheumatic drugs (DMARDs), teriflunomide (**90**) and leflunomide (**91**), considered for po-

tential COVID-19 use. As mentioned before, teriflunomide (**90**) inhibits human DHODH in the low μM range. As anticipated, SF_5-leflunomide **94** was more potent than leflunomide (**91**). SF_5-teriflunomide **93** was approximately twice as active as teriflunomide (**90**). However, an infection inhibition assay showed that none of the compounds had an inhibitory effect against SARS-CoV-2 infection in the infected cells. Nevertheless, the SF_5 analogue of teriflunomide **93** might be a useful DHODH probe molecule for future investigation and could maybe challenge DSM 265 **89** (Figure 5).

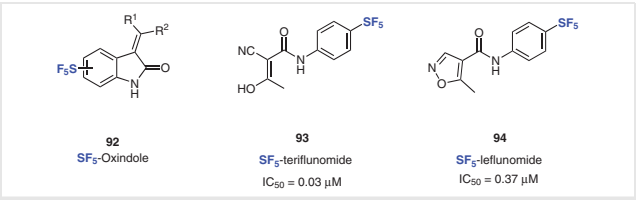

Figure 5 SF_5-teriflunomide and SF_5-leflunomide

Cyclin-dependent kinase 2 (CDK2) has been validated as target for both cancer and contraception but remain highly challenging because of the structural similarity of the ATP-binding site. Thanks to the specific properties of the SF_5 moiety, Georg and co-workers developed a SF_5 analogue named EF-4-177 **95** which showed a greater than tenfold improvement in affinity compared to TW-8-67-2.[44] EF-4-177 **95** leads to the highest affinity compound by ITC of the series (K_D = 7.4 nM) at the sensitivity limit of the instrument. The higher affinity compound EF-4-177 **95** demonstrated a half-life that was greater than eightfold longer in humans and greater than sevenfold longer in mice compared to CF_3 analogue **96** (Figure 6). Additionally, oral administration of EF-4-177 **95** in mice demonstrated a corresponding long exposure in both plasma and specifically testis for contraceptive uses. The overall stability of EF-4-177 **95** with low clearance demonstrated the potential for multiple therapeutic uses that require selective targeting of CDK2 and the potential of this series as oral medications.

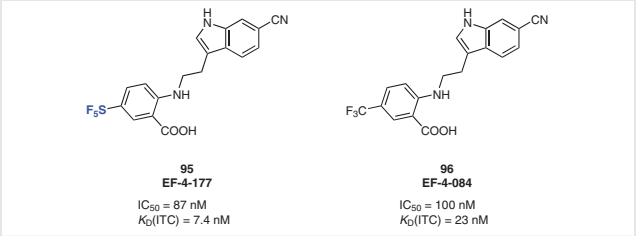

Figure 6 SF_5-analogue of cyclin-dependent kinase 2 CDK2

The NK1 receptor (NK1R) is a molecular target for approved and experimental drugs intended for a variety of conditions, including pain and cancers, and several NK1R antagonists are approved for the prevention of the chemotherapy-induced nausea. In 2023, the Lipinski group examined the replacement the CF_3 groups common for many NK1R ligands with other groups. The specific properties coupled with the nickname 'Super-CF_3' led to the examination of the SF_5 group.[45] Ten SF_5-containing compounds were synthesized and tested for NK1R affinity. All of the ten analogues exhibit NK1R binding affinity and the best of them, **98**, exhibit almost the same activity to aprepitant (**97**) which is the approved NK1R-targeting drug (IC_{50} = 34.4 nM SF_5 vs 27.7 for aprepitant). This is a demonstration of utility of the SF_5 group in the field of NK1R ligands (Figure 7).

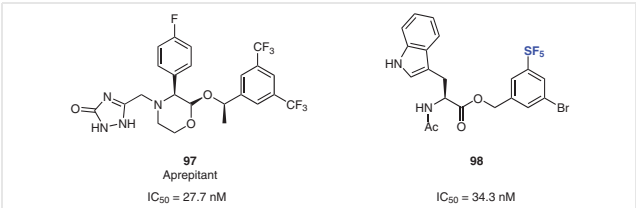

Figure 7 Aprepitant and its SF_5 analogue

In 2023, the Miller group reported on the importance of prodrugs in therapeutic application. A three series of novel lipid prodrugs of TFV were designed and synthesized.[46] These novel prodrugs were evaluated for antiviral activity in HIV pseudoviral assays and for metabolic stability in HLM (human liver microsomes). While detailed intracellular metabolism experiments and *in vivo* pharmacokinetic studies are critical components of future plans, these results also highlighted SF_5 as a complementary tool to CF_3 and $Si(CH_3)_3$ in the growing repertoire of metabolically inert lipid termini. In fact, SF_5 derivatives **100** displayed relevant stability (HLM >120 min), with high HIV activities (IC_{50} = 14.6 nM) very close to an approved nucleotide HIV reverse transcriptase inhibitor analogue: tenofovir exalidex (TXL, **99**) (HLM 42 min; IC_{50} = 18.0 nM) and with similar therapeutic index (>6850 for SF_5-@ vs 5420 for TXL) (Figure 8).

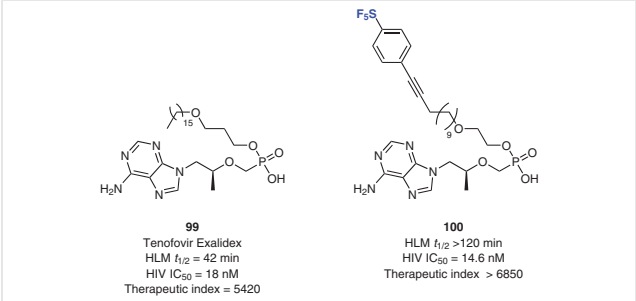

Figure 8 Tenofovir exalidex TXL and its SF_5 analogue

Bassetto and co-workers, in 2023, developed and identified a series of new nucleoside analogues designed to act as inhibitors of human METTL3, as a novel approach to interfere with a range of viral infections.[47] These substrates were evaluated for their ability to interfere with the replication

of different viruses in cell-based assays, with EC_{50} values in the sub-micromolar range. Among the variety of substituent in the series, *meta*-chloro substituent at the benzyl ring showed the best result with a submicromolar EC_{50} against EV71, followed by SF_5 (EV71 EC_{50} = 0.065 μM Cl vs EV71 EC_{50} = 0.102 μM SF_5, respectively). Despite their activities, none of the compounds showed any cytotoxic effect at the test concentrations in both cell lines (Figure 9).

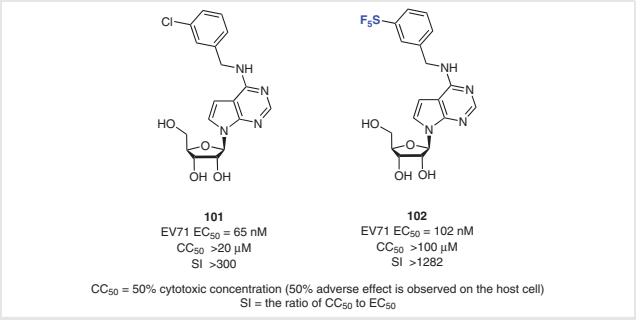

Figure 9 New SF_5 tagged nucleoside analogues as inhibitors of human METTL3

Drug-resistant bacterial pathogens still cause high levels of mortality annually despite the availability of many antibiotics. HSGN-144 **103** was reported in 2020 to have activity against MRSA as well as other drug-resistant Gram-positive strains.[48a] In 2022, the Sintim group showed that this compound also demonstrates high potency against MRSA clinical isolates with a MIC of 0.5 μg/mL (1.3 μM).[48b] Overall, OCF_3, SCF_3, and SF_5 derivatives, performed similarly or better than vancomycin and showed a low propensity to develop resistance to MRSA over 30 days. In addition, it was demonstrated that the three compounds downregulated essential proteins involved in DNA replication and they have significant effect on membrane depolarization but did not alter membrane permeability. HSGN-220 **104**, HSGN-218 **105**, and HSGN-144 **103** are multi-targeting antibiotics that regulate menaquinone biosynthesis and other essential proteins (Figure 10). The mode of action of these compounds is unknown, but iron starvation appears to be part of the mechanism of action that led to bacterial killing.

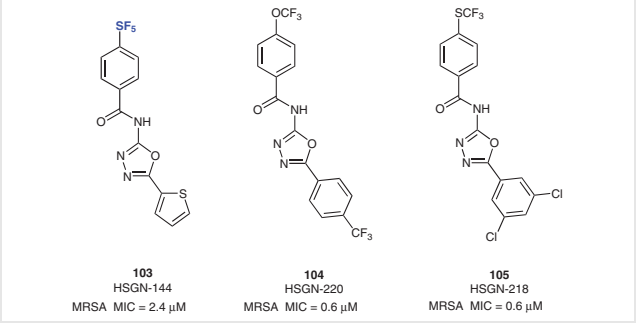

Figure 10 SF_5-, OCF_3-, and SCF_3-based molecules as multi-targeting antibiotics

Conceptually, Turner and co-workers, in 2024, reported the antibacterial efficacy of a novel pentafluorosulfanyl-containing triclocarban analogues against Gram-positive bacteria notably *Staphylococcus aureus*, *Staphylococcus epidermidis*, and MRSA.[49] In this study, twenty new compounds were prepared and tested. The majority of them showed a broad spectrum of antibacterial activity. Interestingly, compounds **106**, **107**, and **108** showed better antibacterial (MIC values) and antibiofilm activity (MBIC values) than ciprofloxacin and gentamycin against *S. aureus*, MRSA, and *S. epidermidis* (Figure 11). Moreover, mechanistic studies as well as cell toxicity have been evaluated and showed promising challenging results that could be optimized.

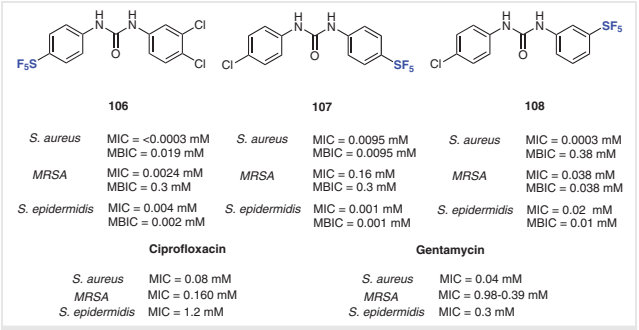

Figure 11 Pentafluorosulfanyl-containing triclocarban analogues

Moreover, the Kawai and co-workers evaluated the optimization of the chemical structure of a bacterial-selective multidrug and toxin extrusion (MATE) inhibitor **109** in order to improve its activity (EC_{50} >30 μM).[50] Structural modifications on each part of this compound (aromatic, linker, and guanidine parts) were performed and the efficacy of the corresponding derivatives was evaluated. Indeed, the presence of the pentafluorosulfanyl group on the aromatic part improved remarkably the activity of the MATE-type inhibitor **110** (Figure 12) against HmrM-expressing strain when co-administrated with norfloxacin (EC_{50} = 1.8 μM). The highest efficacy obtained could be due to the unique properties of the SF_5 group including lipophilicity, bulkiness, and electronegativity, but it is still unclear. Additionally, compound **110** showed no cytotoxicity at effective concentrations, making it a promising MATE-type inhibitor.

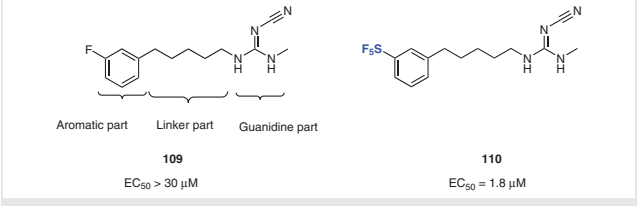

Figure 12 Pentafluorosulfanyl-tagged MATE-type inhibitor

It had been estimated that the majority of human microbial infections are linked to or directly caused by bacterial biofilms and are immune to most currently approved FDA drugs. The Sintim group proposed, in 2022, the development of potent antibiotics against biofilms. It had shown that pentafluorosulfanyl-containing quinoline compounds, kill persister bacteria.[51a] Therefore, the compounds in the library were expanded to increase the diversity of compounds that could be further developed into therapeutics. Thanks to the Povarov reaction, several derived SF_5-containing compounds were synthesized and showed the inhibition of both clinical and laboratory strains of Gram-positive bacteria.[51b] The lead compound, HSD 1919 **111** (Scheme 30) exhibited rapid bactericidal mode of action against multidrug resistant (MDR) staphylococcal and enterococcal strains such as MRSA (eradicated in 2–8 h) and VRE via bacterial membrane disruption at relatively low concentrations (8 μg/mL). Toxicity studies showed that HSD 1919 was nontoxic *in vitro* to mammalian red blood cells at 10X MIC (minimum inhibitory concentration).

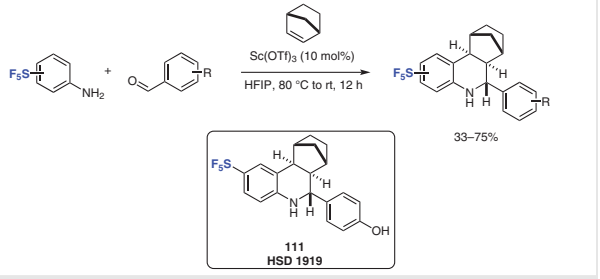

Scheme 30 Synthesis of pentafluorosulfanyl-containing quinoline compounds for antibacterial activity

Tuberculosis is an ancient, but still sinister, disease of global importance. It was shown that imidazo[1,2-*a*]pyridine-3-carboxamides (IAPs) have impressive nanomolar *in vitro* potency against *Mycobacterium tuberculosis* (Mtb) since it was exemplified by clinical candidate telacebec (Q203, **112**). Nevertheless, it suffers from lack of metabolic stability. In order to solve this problem, the Miller group explored, in 2022, deuterated imidazo[1,2-*a*]pyridine-3-carboxamides and their anti-tuberculosis activity.[52] The deuterated analogues showed better metabolic stability as demonstrated by longer half-lives and lower clearance. In this series 4-pentafluorosulfanyl **113** appeared to be the most active compound with low MIC values of 2.2 nM and 2.9 nM against H37RvMtb in GAS media, respectively (5.5 nM and 5.9 nM in 7H12 media, respectively) which compares well with clinical candidate Q203 **112** (MIC = 0.9 nM and 3.6 nM in GAS and 7H12 media, respectively, Figure 13).

SLU-2633 **114** has been demonstrated as a potent lead compound for the identification of treatment for cryptosporidiosis, caused by the parasite *Cryptosporidium* (EC_{50} = 0.17 μM). This compound is potent and orally efficacious,

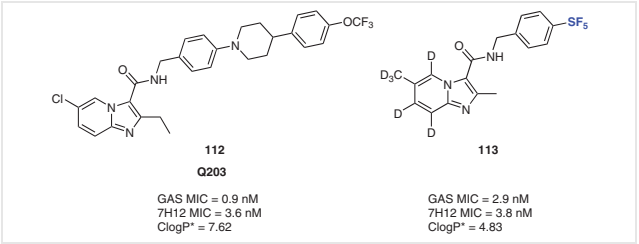

Figure 13 Telacebec and its SF_5 analogue

the mechanism of action and biological target(s) of this series are currently unknown. To solve this problem, the Meyers group developed phenotypic structure-activity relationships around the aryl 'tail' group.[53] They observed that electron-withdrawing groups are preferred over electron-donating groups. In addition, fluorine seems to play a remarkable role in the potency of the molecule. The most potent compound SLU-10482 **115** displayed very good activity (EC_{50} = 0.07 μM) and was found to be orally efficacious. Nevertheless, larger groups such as SF_5 **116** that are also electron-withdrawing lose the advantage that other electron-withdrawing groups give in this special case and appear to be the least effective (Figure 14).

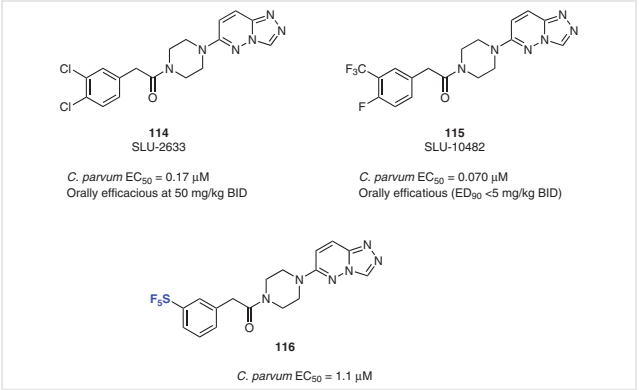

Figure 14 SF_5 analogue of SLU derivatives for the treatment of cryptosporidiosis

Finally, relaxin H2 is a clinically relevant peptide agonist for relaxin family peptide receptor 1 (RXFP1), but this hormone suffers from a short plasma half-life and the need for injectable delivery. These disadvantages limit its therapeutic potential. Granberg and co-workers proposed the development of a potent small molecule RXFP 1 agonist.[54] They discovered compound AZ7976 **118** a highly selective RXFP 1 agonist with sub-nanomolar potency (pEC_{50} = 9.4). At first, it appeared to have good metabolic stability in hHEPs, but it suffered from high clearance, as ML290 **117** the previous lead. Overall, the excellent potency of AZ7976 balanced the poor metabolic stability to a significant extent, and the eD2M (early dose to man) was 60 mg/70 kg/day and greatly below their first target of 500 mg/70 kg/day. It should be

noticed that the other enantiomer of AZ7976 **118** appears to be 10000-fold less potent. As a result, AZ7976 **118** was selected as lead for further optimization (Figure 15).

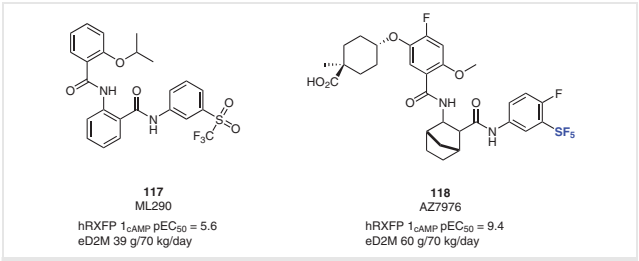

Figure 15 AZ7976 as highly selective RXFP 1 agonist

Long-chain fatty acids substituted by an aryl carbamate have been shown to act as protonophoric mitochondrial uncouplers for the first time by Rawling and co-workers.[55] Prepared in 2 steps from the corresponding anilines **119** (Scheme 31), carbamates such as **120** self-assemble into anionic dimers that are membrane permeable and thus allow proton transport across the mitochondrial inner membrane (MIM). The latter step is the rate-limiting event of the protonophoric cycle. Carbamate **120** possessing a *meta*-SF_5 aromatic is the most efficient derivative in the JC-1 assay, with an IC_{50} in MDA-MB-231 cells of 3.9±0.4 μM.

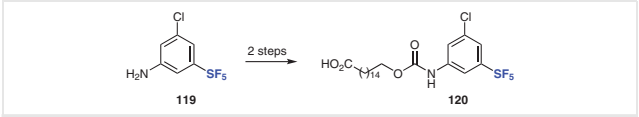

Scheme 31 Synthesis of *meta*-SF_5 aromatic carbamate as a protonophoric mitochondrial uncoupler

Fluorine magnetic resonance imaging (^{19}F MRI) presents several advantages over ^{1}H MRI in obtaining anatomical and physiological images, as fluorine is not an abundant element in the body. Molecular engineering of ^{19}F MRI agents allows for the preparation of selective analyte-responsive compounds. Que and co-workers reported the synthesis of the Fe-complexes Fe($^{II/III}$)DO3A SF_5 **124** and **125**, which possesses a reversible redox sensing ability that is central in monitoring dynamic redox processes.[56] The use of a SF_5-based ligand is unprecedented in biosensing applications. Complex **124** in the Fe^{III} oxidation state shows no ^{19}F MRI signal whereas the addition of one equivalent of cysteine reduces the complex to Fe^{II} which displays a ^{19}F signal. An additional value of the SF_5 motif is that another fluorinated probe (for example containing a CF_3 group) can be simultaneously used for multicolor imaging (Scheme 32).

Other efforts in the fields of ^{19}F MRI and PET imaging were reported by Pascali and co-workers using SF_5-aryl *N*-substituted maleimide and acrylamide which act as [^{18}F]radio-prosthetic groups for bioconjugation.[57] However, the hydrophobicity of the SF_5-tagged compounds significantly limits the application of these bioconjugations in aqueous media.

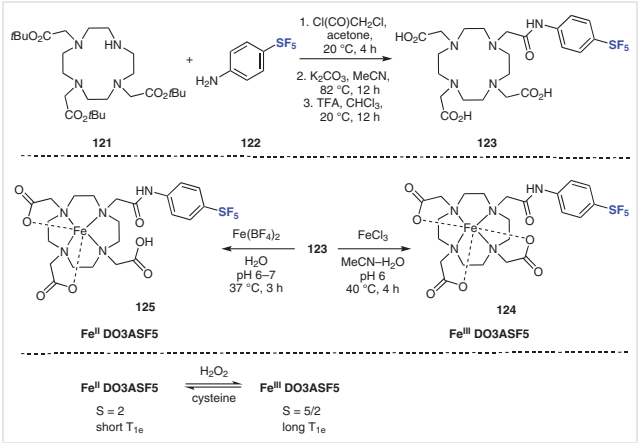

Scheme 32 Synthesis of SF_5-based Fe complex for ^{19}F MRI

3.2 Material Science

The influence of the SF_5 group on the hydrophobic properties of polymethacrylate **128** was studied.[58] The latter was obtained in two steps from methacryloyl chloride (**126**) and *p*-SF_5-phenol, followed by radical polymerization in the presence of AIBN (1 mol%) in THF at 70 °C (Scheme 33). The obtained material possesses a glass transition temperature of 134 °C, superior to the fluorinated material in which the SF_5 group is substituted by a CF_3 (77 °C). This phenomenon was attributed to the steric bulk of the SF_5 group as well as to its increased polarity. The promising hydrophobicity of **128** and of the thin films obtained by spin coating of **128** were studied by surface contact angle and neutron reflectivity measurements.

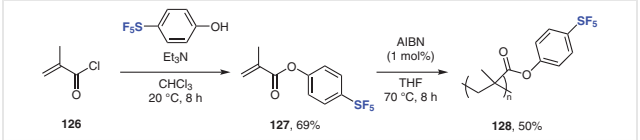

Scheme 33 Synthesis of SF_5-polymethacrylate to evaluate their hydrophobicity

SF_5-substituents have been introduced in BODIPY scaffolds to evaluate their influence on the spectroscopic properties of these dyes, that have found multiple applications in chemistry and biology. Benniston and co-workers reported structural variations either in the *meso* position (**BD1**, **BD2**, **BD4**, and **BD5**) or in the 3,5-positions (**BD6**) of the BODIPY (Figure 16).[59]

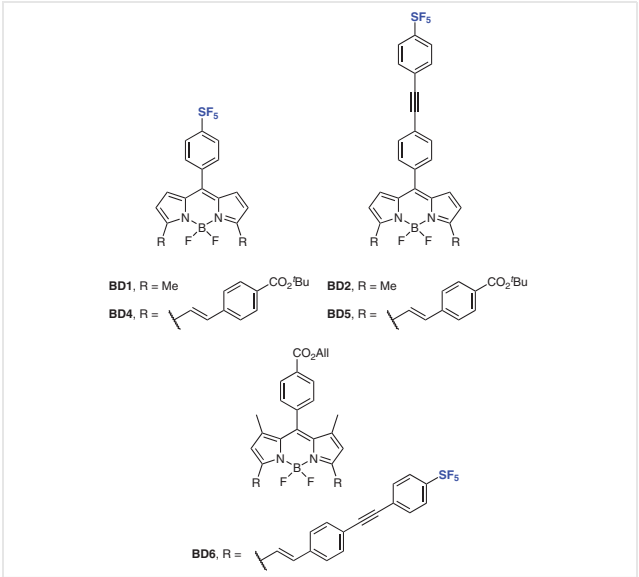

Figure 16 SF_5-tagged BODIPY scaffolds

BD1 and **BD2** possess a strong solid-state emission. In solution, **BD1** exhibits stronger fluorescence quantum yield (0.30) than **BD2** (0.07). This phenomenon was attributed to a greater rigidity of **BD1** (imparted by the negative hyperconjugation and 'no-bond' resonance character of SF_5) which in turn help reduce the nonradiative processes of the first excited singlet state. **BD4–6** are π-conjugated at the 3,5-positions but they do not possess classical solvatochromic properties, which indicates that no charge-transfer transitions take place even with the strongly electron-withdrawing SF_5 motif.

BD1 and **BD4** and its corresponding dicarboxylic acid (**BD4-CO_2H**, able to bind to NiO) were also studied by Gibson and co-workers in tandem dye-sensitized solar cells with a photoactive electrode.[60] Improved properties imparted by the SF_5 substituent originate from the extended charge separation lifetime within the dyes, which reduces recombination and increase current flow. However, molecular design still needs to be improved to deliver dyes that are competitive with the current standard of the field.

Interestingly, pentafluoro(4-nitrophenyl)-λ^6-sulfane has been shown to be a promising fluorinated organic catholyte in lithium primary batteries, allowing 8 electrons to be transferred per molecule. This simple SF_5-aromatic can deliver interesting energy density (1085 Wh kg^{-1}) but a 20% decrease was observed with time.[61] Gallant and co-workers showed that reduction products (fluorinated polysulfide species) were produced along the upper-voltage plateau, and their insolubility at high concentrations of DMSO were problematic.[62]

SF_5-aromatics have been central to the design of a boron-based anion which was shown to impart better stability to organometallic complexes in solid-state transformations. Jenkins, Macgregor, Weller, and co-workers demonstrated that $[B(3,5\text{-}(SF_5)_2C_6H_3)_4]^-$ ([S-$BAr^F{}_4$]) led to a stable microcrystalline rhodium complex [$Rh(Cy_2PCH_2CH_2PCy_2)(NBD)$] [S-$BAr^F{}_4$] thanks to increased non-covalent interactions.[63] Under an atmosphere of dihydrogen, this complex undergoes a single-crystal to single-crystal reaction delivering the corresponding σ-alkane complex.

Self-assemble monolayers (SAMs) anchored on gold surface and exposing a uniform SF_5 surface to ambient were reported by Terfort, Zharnikov, and co-workers.[64] Oligophenylenes were chosen as the linking element between the thiol-anchoring group and the pentafluorosulfanyl motif. The resulting SF_5-BPT **129** (biphenylthiol) and SF_5-TPT **130** (terphenylthiol) demonstrated an exceptional wetting and electrostatic properties in comparison to the analogous trifluoromethylated SAMs (Scheme 34). Of particular interest is the unrivaled value of the work function (close to 6.0 eV) among the SAM-engineered gold substrates.

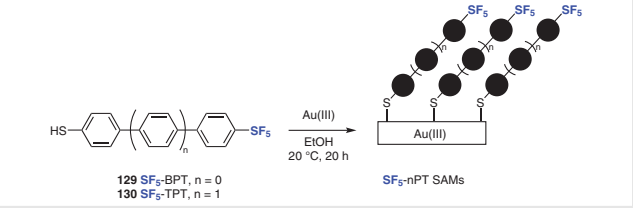

Scheme 34 Synthesis of SF_5 tagged self-assemble monolayers (SAMs) anchored on gold surface

Moreover, the influence of SF_5-substituents on the properties of azo-imidazole based photoswitches was reported by Podlesný, Bureš, and co-workers.[65] Two types of switches were prepared differing by the substitution of the nitrogen atom of the imidazole (NH for **132** and NMe for **133**). The former is conveniently synthesized from *p*-SF_5-aniline **131** by diazotization with sodium nitrite followed by condensation with 1*H*-imidazole while an extra step of *N*-methylation is necessary to deliver **133** (Scheme 35). In photoinduced *E*/*Z* isomerization studies, it was observed that **133** possessed the longest half-life (almost 24 h, twice the value of the corresponding trifluoromethyl analogue) thanks to *N*-methylation which limits tautomerism of the imidazole. In comparison, the $\tau_{1/2}$ of the NH derivative **132** is only 13 s. DFT calculations suggest that intramolecular London dispersion interactions in (*Z*)-**133** between the fluorine atom lone pairs of the SF_5 group and the imidazole contribute to its stabilization.

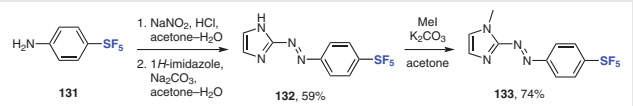

Scheme 35 Synthesis of SF_5 tagged azo-imidazole based photoswitches

3.3 Catalysis

Chiral imidodiphosphorimidate (IDPi) **134a–g** substituted by SF_5 aromatics by the List group, in 2022, have been shown to catalyze diverse type of transformations such as the asymmetric spirocyclizing Diels–Alder reactions of *exo*-enones with dienes (Scheme 36a).[66] This unprecedented cycloaddition is general and proceeds in moderate to good yields with excellent regio- and enantiomeric ratios. In contrast to IDPi, less acidic catalysts (such as phosphoric acids, disulfonimides, imidodiphosphates) did not promote the transformation. This method could be extended to the kinetic resolution of (±)-**135** leading to **136**, a known intermediate en route to (+)-colletoic acid, in 37% yield and excellent regio-, diastereo-, and enantiomeric ratios. DFT calculations were conducted to shed light on the stereochemical outcome of this catalytic Diels–Alder reaction. It was shown that the reaction occurs via an asynchronous concerted transition state, and that the stereoselectivity was primarily controlled by steric factors and more favorable substrate distortion.

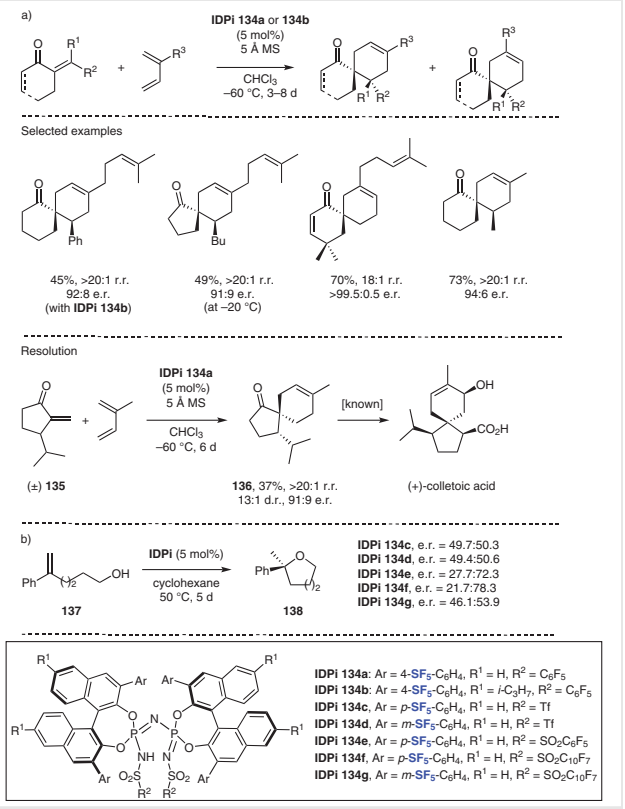

Scheme 36 Catalytic activity of SF_5 substituted chiral imidodiphosphorimidate (IDPi)

In 2023, the List group focused on the *in silico* prediction of the enantioselectivity of IPDi based on tunable fragment descriptors, in two model transformations.[67] One of these transformations is depicted in Scheme 36b and involves the acid-catalyzed intramolecular cyclization of **137** to give the corresponding tetrahydropyran **138**. A machine learning model based on fragment descriptors allowed a virtual screening of IDPi catalysts, including **134c–g** which possess aromatic SF_5 substituents. Although the experimental enantioselectivities were low, an optimal catalyst was eventually predicted and its enantioselectivity was confirmed experimentally (96:4 e.r., not shown). Overall, this approach does not rely on costly quantum mechanical calculations and further demonstrates that ML approaches are able to predict selectivities of catalytic reactions beyond a limited set of data.

In 2024, Spivey, Bull, and co-workers reported the use of a novel and readily accessible SF_5-containing cinchona alkaloid derived phase transfer catalyst (PT) **139** for the enantioselective synthesis of spirocyclic azetidine oxindoles with high yields and with up to 2:98 e.r. outperforming the corresponding CF_3 analogue.[68] The scope of the reaction included electron-poor and electron-rich substituents on the oxindole aryl ring, and also different protecting and leaving groups have also been explored (Scheme 37).

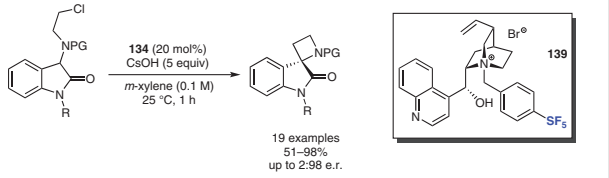

Scheme 37 The enantioselective synthesis of spirocyclic azetidine oxindoles catalyzed by an SF_5-containing cinchona alkaloid derived phase transfer catalyst

4 Conclusion

The chemistry of SF_5 has evolved exponentially over the last three years as summarized herein in this review article. New achievements are closely connected to the crucial use of gaseous SF_5Cl in pentafluorosulfanylation reactions, either from commercial supply, from *in situ* generation, or prepared in stock solution. In addition, recent advances on oxidative fluorination reactions also open doors for a more straightforward access to SF_5-building blocks. This SF_5 motif is of constant growing interest in many fields such as biological and medicinal chemistry, catalysis, and material science. This craze is mainly due to the unique properties of SF_5 in terms of geometry, volume, electronegativity, lipophilicity, and stability. Often compared to the CF_3 group, the SF_5 group is fundamentally different and induces specific reactivity and selectivity that need to be fully understood and supported by computational studies. Many challenges still need to be addressed such as the late-stage introduction of the SF_5 motif and more fundamental studies about the biocompatibility of this perfluorinated motif in life science.

Conflict of Interest

The authors declare no conflict of interest.

Funding Information

This work is supported by the CNRS program Emergence@INC 2023. The authors acknowledge the University of Strasbourg for a doctoral contract to Lucas Popek and CNRS Chimie for post-doctoral contract of Dr Mariam Abd El Sater.

References

(1) Haufe, G. *Tetrahedron* **2022**, *109*, 132656.
(2) Saccomanno, M.; Hussain, S.; O'Connor, N. K.; Beier, P.; Somlyay, M.; Konrat, R.; Murphy, C. D. *Biodegradation* **2018**, *29*, 259.
(3) (a) Silvey, G. A.; Cady, G. H. *J. Am. Chem. Soc.* **1950**, *72*, 3624. (b) Roberts, H. L.; Ray, N. H. *J. Chem. Soc.* **1960**, 665. (c) Sheppard, W. A. *J. Am. Chem. Soc.* **1960**, *82*, 4751.
(4) Ait-Mohand, S.; Dolbier, W. R. *Org. Lett.* **2002**, *4*, 3013.
(5) Savoie, P. R.; Welch, J. T. *Chem. Rev.* **2015**, *115*, 1130.
(6) (a) Sani, M.; Zanda, M. *Synthesis* **2022**, *54*, 4184. (b) Kordnezhadian, R.; Li, B.-Y.; Zogu, A.; Demaerel, J.; De Borggraeve, W. M.; Ismalaj, E. *Chem. Eur. J.* **2022**, *28*, e202201491. (c) Magre, M.; Ni, S.; Cornella, J. *Angew. Chem. Int. Ed.* **2022**, *61*, e202200904. (d) Rombach, D.; Wagenknecht, H.-A. *Synthesis* **2022**, *54*, 4883. (e) Kraemer, Y.; Bergman, E. N.; Togni, A.; Pitts, C. R. *Angew. Chem. Int. Ed.* **2022**, *61*, e202205088.
(7) Birepinte, M.; Champagne, P. A.; Paquin, J.-F. *Angew. Chem. Int. Ed.* **2022**, *61*, e202112575.
(8) Ouellet-Du Berger, M.-R.; Boucher, M.; Paquin, J.-F. *J. Fluorine Chem.* **2023**, *268*, 11013.
(9) Shou, J.-Y.; Xu, X.-H.; Qing, F.-L. *J. Fluorine Chem.* **2022**, *261-262*, 110018.
(10) Shou, J.-Y.; Xu, X.-H.; Qing, F.-L. *Angew. Chem. Int. Ed.* **2021**, *60*, 15271.
(11) Shou, J.-Y.; Qing, F.-L. *Angew. Chem. Int. Ed.* **2022**, *61*, e202208860.
(12) Nguyen, T. M.; Legault, C. Y.; Blanchard, N.; Bizet, V.; Cahard, D. *Chem. Eur. J.* **2023**, *29*, e202302914.
(13) Nguyen, T. M.; Popek, L.; Matchavariani, D.; Blanchard, N.; Bizet, V.; Cahard, D. *Org. Lett.* **2024**, *26*, 365.
(14) Wang, L.; Qin, W. *Org. Lett.* **2024**, *26*, 5049.
(15) Kraemer, Y.; Ghiazza, C.; Ragan, A. N.; Ni, S.; Lutz, S.; Neumann, E. K.; Fettinger, J. C.; Nöthling, N.; Goddard, R.; Cornella, J.; Pitts, C. R. *Angew. Chem. Int. Ed.* **2022**, *61*, e202211892.
(16) Zhao, X.; Shou, J.-Y.; Qing, F.-L. *Sci. China. Chem.* **2023**, *66*, 2871.
(17) Kraemer, K.; Buldt, J. A.; Kong, W.-Y.; Stephens, A. M.; Ragan, A. N.; Park, S.; Haidar, Z. C.; Patel, A. H.; Shey, R.; Dagan, R.; McLoughlin, C. P.; Fettinger, J. C.; Tantillo, D.; Pitts, C. R. *Angew. Chem. Int. Ed.* **2024**, *63*, e202319930.
(18) Wozniak, M.; Sander, S.; Cula, B.; Ahrens, M.; Braun, T. *Chem. Eur. J.* **2022**, *28*, e202200626.
(19) Pitts, C. R.; Santschi, N.; Togni, A. WO 2019229103, **2019**.
(20) Kordnezhadian, R.; De Bels, T.; Su, K.; Van Meervelt, L.; Ismalaj, E.; Demaerel, J.; De Borggraeve, W. M. *Org. Lett.* **2023**, *25*, 8947.
(21) Taponard, A.; Jarrosson, T.; Khrouz, L.; Médebielle, M.; Broggi, J.; Tlili, A. *Angew. Chem. Int. Ed.* **2022**, *61*, e202204623.
(22) (a) Umemoto, T.; Lloyd, M.; Garrick, L. M.; Saito, N. *Beilstein J. Org. Chem.* **2012**, *8*, 461. (b) Pitts, C. R.; Bornemann, D.; Liebing, P.; Santschi, N.; Togni, A. *Angew. Chem. Int. Ed.* **2019**, *58*, 1950. (c) Cui, B.; Kosobokov, M.; Matsuzaki, K.; Tokunaga, E.; Shibata, N. *Chem. Commun.* **2017**, *53*, 5997. (d) Wang, L.; Cornella, J. *Angew. Chem. Int. Ed.* **2020**, *59*, 23510. (e) Wang, L.; Ni, S.; Cornella, J. *Synthesis* **2021**, *53*, 4308.
(23) Gatzenmeier, T.; Liu, Y.; Akamatsu, M.; Okazoe, T.; Nozaki, K. *ChemRxiv* **2023**, preprint DOI: 10.26434/chemrxiv-2023-jzn11.
(24) Kordnezhadian, R.; Zogu, A.; Borgarelli, C.; Van Lommel, R.; Demaerel, J.; De Borggraeve, W. M.; Ismalaj, E. *Chem. Eur. J.* **2023**, *29*, e202300361.
(25) Popek, L.; Nguyen, T. M.; Blanchard, N.; Cahard, D.; Bizet, V. *Tetrahedron* **2022**, *117–118*, 132814.
(26) Paquin, P.; DeGrâce, N.; Bélanger-Chabot, G.; Paquin, J.-F. *J. Org. Chem.* **2024**, *89*, 3552.
(27) Popek, L.; Cabrera-Trujillo, J. J.; Debrauwer, V.; Blanchard, N.; Miqueu, K.; Bizet, V. *Angew. Chem. Int. Ed.* **2023**, *62*, e202300685.
(28) Wenzel, J. O.; Jester, F.; Togni, A.; Rombach, D. *Chem. Eur. J.* **2024**, *30*, e202304015.
(29) Kucher, H.; Wenzel, J. O.; Rombach, D. *ChemPlusChem* **2024**, *89*, e202400168.
(30) Murata, Y.; Hada, K.; Aggarwal, T.; Escorihuela, J.; Shibata, N. *Angew. Chem. Int. Ed.* **2024**, *63*, e202318086.
(31) Matchavariani, D.; Popek, L.; Cabrera-Trujillo, J. J.; Nguyen, T. M.; Blanchard, N.; Miqueu, K.; Cahard, D.; Bizet, V. *Adv. Synth. Catal.* **2024**, *366*, 3481.
(32) Köring, L.; Stepen, A.; Birenheide, B.; Barth, S.; Leskov, M.; Schoch, R.; Krämer, F.; Breher, F.; Paradies, J. *Angew. Chem. Int. Ed.* **2023**, *62*, e202216959.
(33) Le, T. V.; Daugulis, O. *Chem. Commun.* **2022**, *58*, 537.
(34) Michaut, A.; Quatrevaux, S.; Queguiner, L.; Gaurrand, S.; Guillemont, J. *Lett. Org. Chem.* **2022**, *19*, 602.
(35) Mastalerz, V.; Lam, K.; Paquin, J.-F. *J. Fluorine Chem.* **2023**, *268*, 110113.
(36) Peyrical, L. C.; Ouellet-Du Berger, M.-R.; Boucher, M.; Birepinte, M.; Paquin, J.-F.; Charette, A. B. *Org. Lett.* **2023**, *25*, 2487.
(37) Dudziński, P.; Matsnev, A. V.; Trasher, J. S.; Haufe, G. *J. Fluorine Chem.* **2022**, *264*, 110051.
(38) Ghosh, H.; Bhattacharyya, S.; Schobert, R.; Dandawate, P.; Biersack, B. *Pharmaceutics* **2023**, *15*, 1921.
(39) Kaps, L.; Klefenz, A.; Traenckner, H.; Schneider, P.; Andronache, I.; Schobert, R.; Biersack, B.; Schuppan, D. *Cells* **2023**, *12*, 2619.
(40) Karaj, E.; Dlamini, S.; Koranne, R.; Sindi, S. H.; Perera, L.; Taylor, W. R.; Viranga Tillekeratne, L. M. *Bioorg. Chem.* **2022**, *122*, 105700.
(41) Scortichini, M.; Mohammed Idris, R.; Moschütz, S.; Keim, A.; Salmaso, V.; Dobelmann, C.; Oliva, P.; Losenkova, K.; Irjala, H.; Vaittinen, S.; Sandholm, J.; Yegutkin, G. G.; Sträter, N.; Junker, A.; Müller, C. E.; Jacobson, K. A. *J. Med. Chem.* **2022**, *65*, 2409.
(42) Pontikos, M. A.; Leija, C.; Zhao, Z.; Wang, X.; Kilgore, J.; Tornesi, B.; Adenmatten, N.; Phillips, M.; Williams, N. *Biochem. Pharmacol.* **2022**, *204*, 115237.
(43) Jose, A.; Guest, D.; LeGay, R.; Tizzard, G. J.; Coles, S. J.; Derveni, M.; Wright, E.; Marrison, L.; Lee, A. A.; Morris, A.; Robinson, M.; von Delft, F.; Fearon, D.; Koekemoer, L.; Matviuk, T.; Aimon, A.; Schofiled, C. J.; Malla, T. R.; London, N.; Greenland, B. W.; Bagley, M. C.; Spencer, J. *ChemMedChem* **2022**, *17*, e2021006.
(44) Faber, E. B.; Wang, N.; John, K.; Sun, L.; Wong, H. L.; Burban, D.; Francis, R.; Tian, D.; Hong, K. H.; Yang, A.; Wang, L.; Elsaid, M.; Khalid, H.; Levinson, N. M.; Schonbrunn, E.; Hawkinson, J. E.; Georg, G. I. *J. Med. Chem.* **2023**, *66*, 1928.

(45) Witoszka, K.; Malalinska, J.; Misicka, A.; Lipinski, P. F. J. *ChemMedChem* **2023**, *18*, e202300315.
(46) Toti, K. S.; Pribut, N.; D'Erasmo, M.; Dasari, M.; Sharma, S. K.; Bartsch, P. W.; Burton, S. L.; Gold, H. B.; Bushnev, A.; Derdeyn, C. A.; Basson, A. E.; Liotta, D. C.; Miller, E. J. *Front. Pharmacol.* **2023**, *13*, 1083284.
(47) Salerno, M.; Varricchio, C.; Bevilacqua, F.; Jochmans, D.; Neyts, J.; Brancale, A.; Ferla, S.; Bassetto, M. *Eur. J. Med. Chem.* **2023**, *246*, 114942.
(48) (a) Naclerio, G. A.; Abutaleb, N. S.; Onyedibe, K. I.; Seleem, M. N.; Sintim, H. O. *RSC Med. Chem.* **2020**, *11*, 102. (b) Naclerio, G. A.; Onyedibe, K. I.; Karanja, C. W.; Aryal, U. K.; Sintim, H. O. *ACS Infect. Dis.* **2022**, *8*, 865.
(49) Pormohammad, A.; Moradi, M.; Hommes, J. W.; Pujol, E.; Naesens, L.; Vázquez, S.; Surewaard, B. G. J.; Zarei, M.; Vazquez-Carrera, M.; Turner, R. J. *Microbiol. Spectrum* **2024**, *12*, e00071–24.
(50) Shinya, S.; Kawai, K.; Kobayashi, N.; Karuo, Y.; Tarui, A.; Sato, K.; Otsuka, M.; Omote, M. *Bioorg. Med. Chem.* **2024**, *99*, 117606.
(51) (a) Onyedibe, K. I.; Dayal, N.; Sintim, H. O. *RSC Med. Chem.* **2021**, *12*, 1879. (b) Dayal, N.; Onyedibe, K. I.; Gribble, W. M.; Sintim, H. O. *Eur. J. Med. Chem.* **2022**, *240*, 114550.
(52) Liu, R.; Marshall, K.; Ma, R.; Lien Thi Pham, K.; Shetye, G.; Liu, Z.; Cho, S.; Jeong, H.; Franzblau, S. G.; Moraski, G. C.; Miller, M. J. *Bioorg. Chem.* **2022**, *128*, 106074.
(53) Schubert, T. J.; Oboh, E.; Pekk, H.; Philo, E.; Teixeira, J. E.; Stebbins, E. E.; Miller, P.; Oliva, J.; Sverdrup, F. M.; Griggs, D. W.; Huston, C. D.; Meyers, M. J. *J. Med. Chem.* **2023**, *66*, 7834.
(54) Granberg, K. L.; Sakamaki, S.; Fuchigami, R.; Niwa, Y.; Fujio, M.; Kato, H.; Bergström, F.; Larsson, N.; Persson, M.; Villar, I. C.; Fujita, T.; Sugikawa, E.; Althage, M.; Yano, N.; Yokoyama, Y.; Kimura, J.; Lal, M.; Mochida, H. *J. Med. Chem.* **2024**, *67*, 4442.
(55) MacDerott-Opeskin, H.; Clarke, C.; Wu, X.; Roseblade, A.; York, E.; Pacchini, E.; Roy, R.; Cranfield, C.; Gale, P. A.; O'Mara, M. L.; Murray, M.; Rawling, T. *Org. Biomol. Chem.* **2023**, *21*, 132.
(56) Kadakia, R. T.; Ryan, R. T.; Cooke, D. J.; Que, E. L. *Chem. Sci.* **2023**, *14*, 5099.
(57) Hiscocks, H. G.; Pascali, G.; Ung, A. T. *AppliedChem* **2023**, *3*, 256.
(58) Xie, Y.; Iwata, J.; Matsumoto, T.; Yamada, N. L.; Nemoto, F.; Seto, H.; Nishino, T. *Langmuir* **2022**, *38*, 6472.
(59) James, R. D.; Cucinotta, F.; Waddell, P. G.; Benniston, A. C. *New J. Chem.* **2023**, *47*, 8451.
(60) James, R. D.; Alqahtani, L. S.; Mallows, J.; Flint, H. V.; Waddell, P. G.; Woodford, O. J.; Gibson, E. A. *Sustainable Energy Fuels* **2023**, *7*, 1494.
(61) Gao, H.; Sevilla, A. R.; Hobold, G. M.; Melemed, A. M.; Guo, R.; Jones, S. C.; Gallant, B. M. *Proc. Natl. Acad. Sci. U. S. A.* **2022**, *119*, e2121440119.
(62) Sevilla, A. R.; Gao, H.; Steinberg, K. J.; Gallant, B. M. *J. Phys. Chem. C* **2023**, *127*, 1722.
(63) Doyle, L. R.; Thomson, E. A.; Burnage, A. L.; Whitwood, A. C.; Jenkins, H. T.; Macgregor, S. A.; Weller, A. S. *Dalton Trans.* **2022**, *51*, 3661.
(64) Liu, Y.; Zeplichal, M.; Katzbach, S.; Wiesner, A.; Das, S.; Terfort, A.; Zharnikov, M. *Nano Res.* **2023**, *16*, 7991.
(65) Jelínková, V.; Dellai, A.; Vachtlová, M.; Fecková, M.; Podlesný, J.; Klikar, M.; Castet, F.; Růžička, A.; Pařík, P.; Pytela, O.; Bureš, F. *J. Photochem. Photobiol., A* **2024**, *449*, 115390.
(66) Ghosh, S.; Erchinger, J. E.; Maji, R.; List, B. *J. Am. Chem. Soc.* **2022**, *144*, 6703.
(67) Tsuji, N.; Sidorov, P.; Zhu, C.; Nagata, Y.; Gimadiev, T.; Varnek, A.; List, B. *Angew. Chem. Int. Ed.* **2023**, *62*, e202218659.
(68) Boddy, A. J.; Sahay, A. K.; Rivers, E. L.; White, A. J. P.; Spivey, A. C.; Bull, J. A. *Org. Lett.* **2024**, *26*, 2079.